

AD-A112 220

ELECTRONICS RESEARCH LAB ADELAIDE (AUSTRIA)  
RETROREFLECTIVE PHASE RETARDATION PRISMS. (U)  
JUN 81 J R VENNING

F/G 20/6

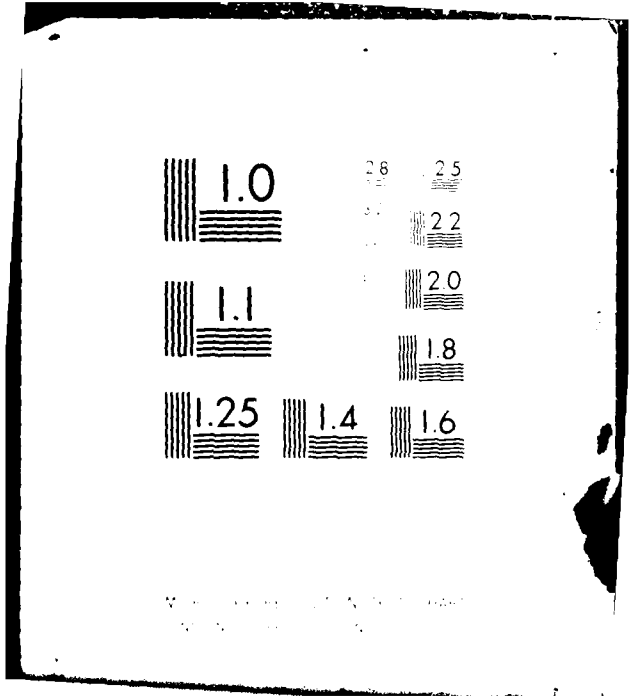
UNCLASSIFIED

ERL-0202-TR

NL

DA  
AD-A  
19220

END  
DATE  
FILMED  
104-82  
DTIC



1.0

2.8 2.5

3.2 2.2

1.1

2.0

1.8

1.25

1.4

1.6

National Bureau of Standards  
NBS Special Publication 300-107

12

ERL-0202-TR

AR-002-593



# DEPARTMENT OF DEFENCE

DEFENCE SCIENCE AND TECHNOLOGY ORGANISATION

ELECTRONICS RESEARCH LABORATORY

DEFENCE RESEARCH CENTRE SALISBURY  
SOUTH AUSTRALIA

## TECHNICAL REPORT

ERL-0202-TR

### RETROREFLECTIVE PHASE RETARDATION PRISMS

J.R. VENNING

DTIC  
RECEIVED  
MAR 19 1982  
H

ADA112220

FILE COPY

Approved for Public Release

COPY No.

JUNE 1981

82 03 20 064

UNCLASSIFIED

12

AR-002-595

DEPARTMENT OF DEFENCE  
DEFENCE SCIENCE AND TECHNOLOGY ORGANISATION  
ELECTRONICS RESEARCH LABORATORY

TECHNICAL REPORT

ERL-0202-TR

RETROREFLECTIVE PHASE RETARDATION PRISMS

J.R. Venning

S U M M A R Y

A retroreflecting device with controlled phase retardation can be made by coating each reflecting surface of a porro prism with a single dielectric film. The amount of phase retardation is a function of the refractive index of the prism, the refractive index of the film and the film thickness. The retardation introduced can be readily controlled in the range of zero to  $\pi$  radians using readily available materials. The materials used are not birefringent. Two phase retardation prisms have been made and evaluated.



DTIC

---

POSTAL ADDRESS: Chief Superintendent, Electronics Research Laboratory,  
Box 2151, GPO, Adelaide, South Australia, 5001

---

UNCLASSIFIED

TABLE OF CONTENTS

	Page No.
1. INTRODUCTION	1
2. REFLECTION FROM UNCOATED SURFACES	1
3. REFLECTION FROM COATED SURFACES	3
3.1 Total reflection at film/external medium interface	3
3.2 Total reflection at incidence medium/film interface	5
3.3 Control of phase difference	6
4. SELECTION OF DESIGN FOR RETROREFLECTIVE WAVEPLATE AT 1.06 $\mu\text{m}$ WAVELENGTH	7
4.1 Selected design of prism with $0^\circ$ phase difference per reflection	8
4.2 Selected design of prism with $90^\circ$ phase difference per reflection	8
5. EVALUATION OF COATED PRISMS	8
5.1 Method of measurement	8
5.2 Measurement of phase difference	9
5.3 Prism coated with magnesium fluoride	10
5.4 Prism coated with titanium dioxide	10
5.5 Discussion of results	10
6. CONCLUSION	11
NOTATION	12
REFERENCES	13

Accession No.	
NTIS ORAI	<input checked="" type="checkbox"/>
DDIC REP	<input type="checkbox"/>
Unannounced	<input type="checkbox"/>
Justification	
By	
Distribution	
Approved for release	
Date	



A

LIST OF FIGURES

1. Single surface reflection
2. Amplitude reflection coefficients as a function of angle of incidence ( $n_1 > n_2$ )
3. Phase change on reflection as a function of angle of incidence ( $n_1 > n_2$ )
4. Amplitude reflection coefficients as a function of angle of incidence ( $n_1 < n_2$ )
5. Phase change on reflection as a function of angle of incidence ( $n_1 < n_2$ )

6. Porro prism
7. Phase change on reflection at  $45^\circ$  angle of incidence as a function of refractive index
8. Total reflection from a coated surface
9. Phase angles for  $n_2 = 2.5$ ,  $n_3 = 1.5$ ,  $AI = 45^\circ$
10. Phase angles for  $n_2 = 1.6$ ,  $n_3 = 1.8$ ,  $AI = 45^\circ$
11. Phase angles for  $n_2 = 1.35$ ,  $n_3 = 1.8$ ,  $AI = 45^\circ$
12. Phase angles for  $n_2 = 1.35$ ,  $n_3 = 2.0$ ,  $AI = 45^\circ$
13. Phase angles for  $n_2 = 1.35$ ,  $n_3 = 4.0$ ,  $AI = 45^\circ$
14. Variation of phase difference with variation of prism index; film index = 1.35, angle of incidence =  $45^\circ$
15. Variation of phase difference with variation of prism index; film index = 2.2, angle of incidence =  $45^\circ$
16. Variation of phase difference with variation of film index; prism index = 1.5, angle of incidence =  $45^\circ$
17. Retroreflective mirror and quarter waveplate retarder
18. Retroreflecting porro prism retarder;  $0^\circ$  phase difference per reflection
19. Retroreflecting porro prism retarder;  $90^\circ$  phase difference per reflection
20. Variation of phase difference with variation of prism index; film index = 1.38, angle of incidence =  $45^\circ$
21. Critical angle of materials in air
22. Variation of phase difference with variation of angle of incidence; prism index = 1.79, film index = 1.38
23. Variation of phase difference with variation of angle of incidence; prism index = 1.45, film index = 2.20
24. Variation of phase difference with variation of angle of incidence; prism index = 1.50, film index = 2.27
25. Layout of measurement system
26. Variation of phase difference with variation of angle of incidence; prism index = 1.76, film index = 1.38
27. Variation of phase difference with variation of angle of incidence; prism index = 1.45, film index = 2.2

## 1. INTRODUCTION

Electro optic systems and devices are increasing in number and complexity and many of these devices rely for their effectiveness on the polarisation properties of light. Many optical devices for use in the fields of illumination, microscopy, lasers, data processing and the measurement of optical properties of materials have been developed to take advantage of the special characteristics of polarised light. Phase retardation devices known as waveplates are used as a means of controlling and changing the state of polarisation of polarised light. Waveplates for use in the visible and near infrared region of the spectrum are generally made of birefringent materials. In special circumstances, and in infrared regions where suitable birefringent materials are not available, reflecting waveplates are required.

The purpose of this report was to investigate the polarisation characteristics of retroreflective porro prisms and any beneficial effects obtainable by coating the reflecting surfaces with thin dielectric films. It was also proposed to apply this work to the design of a retroreflecting porro prism with specific phase retardation characteristics to be used in the resonant cavity of a 1.064  $\mu\text{m}$  laser. This report shows that it is possible to coat the reflecting surfaces of a porro prism so that incident plane polarised light is reflected as plane polarised light with the plane of polarisation at right angles to that of the incident beam. The use of such a prism in the laser resonator has operational and performance advantages. The coated prism described above is a reflecting half waveplate.

In addition the results of this investigation show that the phase difference between the orthogonal components of both visible and infrared radiation reflected at  $45^\circ$  from a single coated surface can be varied from values less than zero to values greater than  $\pi/2$  radians. These results can be applied to other situations where reflecting waveplates are required for controlling or modifying the state of polarisation of polarised light. With the application of a thin film coating to reflecting surfaces the resultant phase difference can be changed in a predictable manner and hence devices such as reflecting or retroreflecting zero, quarter and half waveplates can be made.

Two prisms have been coated and evaluation of these prisms show that the predicted phase control is readily achievable.

## 2. REFLECTION FROM UNCOATED SURFACES

The Fresnel amplitude reflection coefficients applicable to the boundary between two media are (see figure 1)

$$r_p = \frac{n_2 \cos \phi_1 - n_1 \cos \phi_2}{n_2 \cos \phi_1 + n_1 \cos \phi_2}$$
$$r_s = \frac{n_2 \cos \phi_2 - n_1 \cos \phi_1}{n_2 \cos \phi_2 + n_1 \cos \phi_1}$$

where  $n_1$ ,  $n_2$  are the refractive indices of the two media,

p is the subscript specifying that the electric vector is in the plane of incidence

s is the subscript specifying that the electric vector is perpendicular to the plane of incidence

and  $\phi_1$  and  $\phi_2$  the angles in the media, are related by Snell's law

$$n_1 \sin \phi_1 = n_2 \sin \phi_2 .$$

The cosines can be calculated for all values of sine from

$$\cos \phi_1 = \sqrt{1 - \sin^2 \phi_1}$$

$$\cos \phi_2 = \sqrt{1 - \sin^2 \phi_2}$$

The phase change occurring on reflection can be determined from the reflection coefficients by considering

$$r_p = |r_p| \exp(i\delta_p)$$

and

$$r_s = |r_s| \exp(i\delta_s)$$

where  $\delta_p$  and  $\delta_s$  are the phase changes relative to the incident beam.

Considering the reflection from a dielectric material of higher refractive index than the incident medium; (see figures 2 and 3 and reference 1)

$$\delta_s = \pi \text{ for all angles of incidence,}$$

$$\delta_p = 0 \text{ for angles of incidence less than the Brewster angle,}$$

$$\delta_p = \pi \text{ for angles of incidence greater than the Brewster angle,}$$

$$|r_p| = 0 \text{ at the Brewster angle.}$$

For reflection from a dielectric material of lower refractive index than the incident medium (see figures 4 and 5 and reference 1)

$$\delta_s = 0 \text{ and } \delta_p = \pi \text{ for angles of incidence less than the Brewster angle}$$

$$|r_p| = 0 \text{ at the Brewster angle}$$

$$\delta_s = 0 \text{ and } \delta_p = 0 \text{ for angles of incidence between the Brewster angle and the critical angle}$$

$$|r_p| \text{ increases from 0 to 1 for angles of incidence between the Brewster angle and the critical angle}$$

$$|r_s| = |r_p| = 1 \text{ for angles of incidence greater than the critical angle}$$



- $\cos \phi_1 = 0$  at the critical angle
- $\cos \phi_1$  is imaginary for angles of incidence greater than the critical angle
- $\delta_s$  and  $\delta_p$  increase from 0 to  $\pi$  for increasing angles of incidence greater than the critical angle
- $\delta_p = 2\delta_s$  at  $45^\circ$  angle of incidence

The difference in phase,  $\delta = \delta_p - \delta_s$ , is a function of angle of incidence. In the region of total internal reflection  $\delta_p$  and  $\delta_s$  can be calculated from

$$\tan \frac{\delta_p}{2} = \frac{n_2 \sqrt{n_2^2 \sin^2 \phi_2 - 1}}{\cos \phi_2}$$

$$\tan \frac{\delta_s}{2} = \frac{\sqrt{n_2^2 \sin^2 \phi_2 - 1}}{n_2 \cos \phi_2}$$

$$\tan \frac{\delta}{2} = \tan \left( \frac{\delta_p}{2} - \frac{\delta_s}{2} \right) = \frac{\cos \phi_2 \sqrt{n_2^2 \sin^2 \phi_2 - 1}}{n_2 \sin^2 \phi_2}$$

where the outside medium is air(ref.1-3).

In the region of total internal reflection it is possible to control the phase difference between the s and p components by selection of the appropriate glass type and angle of incidence. Several retardation devices based on this principle are described by Bennett and Bennett in reference 2. All but one device in this reference are for in line use, the exception is the Mooney prism which has an angle of  $300^\circ$  between input and output beams. The simple porro prism (figure 6) of refractive index  $n = 1.554$  introduces a  $45^\circ$  phase difference for each reflection and therefore can be considered as a retroreflecting quarter waveplate. The relationship of phase difference  $\delta = \delta_p - \delta_s$  as a function of glass refractive index in air at  $45^\circ$  angle of incidence is shown in figure 7.

Elliptically polarised light produced when plane polarised light is incident on the prism is left or right handed depending on the azimuth of the plane of polarisation of the incident beam with respect to the prism. "Light" has been used in this report as a general term to refer to electromagnetic radiation in the ultraviolet, visible and infrared regions of the electromagnetic spectrum.

### 3. REFLECTION FROM COATED SURFACES

#### 3.1 Total reflection at film/external medium interface

The addition of a dielectric film to the surface of a material used in the totally internal reflecting mode, (see figure 8), modifies the phase terms of the reflection coefficients. Provided that total internal reflection does

not take place at the material/film interface the critical angle is unchanged because the Snell's law relationships between the first and last media are unchanged. Interference effects occur within the film, the resultant amplitudes of the reflection coefficients remain equal to unity and the resultant phase angles depend on the thickness of the film and the angle of incidence. The phase changes,  $\delta_p$  and  $\delta_s$ , and the phase difference  $\delta$  for an angle of incidence of  $45^\circ$  are shown for various combinations of refractive indices in figures 9, 10 and 11. The general behaviour of  $\delta$ ,  $\delta_p$  and  $\delta_s$  can be seen from these figures. Both  $\delta_p$  and  $\delta_s$  tend to large negative values as the film thickness increases, ie extra film thickness introduces a phase delay. Both exhibit an oscillatory component with  $\delta_s$  having the larger perturbations. The phase difference  $\delta$  is oscillatory with respect to increasing film thickness, the amplitude and initial direction of this oscillation depending on the refractive indices of the three materials involved. The optical thickness of the film is calculated in a direction normal to the film and displayed in wavelength units.

The formulae for calculation of the amplitude reflection coefficients are described in most papers introducing thin film theory(ref.4-7) and the following formulae are consistent with reference 8. The angles of incidence and refraction of the light path are related by Snell's law (see figure 8).

$$n_3 \sin \phi_3 = n_2 \sin \phi_2 = n_1 \sin \phi_1$$

$$\text{ie } \sin \phi_2 = \frac{n_3}{n_2} \sin \phi_3$$

and

$$\sin \phi_1 = \frac{n_3}{n_1} \sin \phi_3$$

$$\cos \phi_2 = \sqrt{1 - \sin^2 \phi_2}$$

$$\cos \phi_1 = \sqrt{1 - \sin^2 \phi_1}$$

where  $n_1$ ,  $n_2$ ,  $n_3$  are the refractive indices of the external medium, film and incident medium respectively.  $\phi_1$ ,  $\phi_2$  and  $\phi_3$  are the refracted and incident angles as shown in figure 8.

Because total reflection at interface 2 is being considered the angle  $\phi_1 = 90^\circ$ . The value of  $\sin \phi_1$  when calculated from Snell's law for this condition is equal to or greater than unity. Hence the calculated cosine of  $\phi_1$  is imaginary. Vasicek(ref.9) shows that the imaginary component of  $\cos \phi_1$  must be negative for the evanescent wave in medium 1 to decay exponentially with distance and therefore

$$\cos \phi_1 = -i \sqrt{|1 - \sin^2 \phi_1|}$$

The Fresnel reflection coefficients are

$$r_{2p} = \frac{n_2 \cos \phi_1 - n_1 \cos \phi_2}{n_2 \cos \phi_1 + n_1 \cos \phi_2}$$

$$r_{3p} = \frac{n_3 \cos \phi_2 - n_2 \cos \phi_3}{n_3 \cos \phi_2 + n_2 \cos \phi_3}$$

$$r_{2s} = \frac{n_2 \cos \phi_2 - n_1 \cos \phi_1}{n_2 \cos \phi_2 + n_1 \cos \phi_1}$$

$$r_{3s} = \frac{n_3 \cos \phi_3 - n_2 \cos \phi_2}{n_3 \cos \phi_3 + n_2 \cos \phi_2}$$

where the suffixes on r refer to the interface and the polarisation for which the coefficient is applicable.

Summing the amplitude reflections and omitting the polarisation subscripts the amplitude reflection coefficients for the single film are given by;

$$r = \frac{r_3 + r_2 \exp(-2i \delta_2)}{1 + r_2 r_3 \exp(-2i \delta_2)}$$

where

$$\delta_2 = \frac{2\pi}{\lambda} n_2 d_2 \cos \phi_2$$

$$d_2 = \text{physical thickness of film}$$

and  $\delta_2$  is called the phase thickness of the film.

The reflection coefficients  $r_p$  and  $r_s$  for the film are complex and can be expressed in the form  $r_p = |r_p| \exp(i\delta_p)$

$$r_s = |r_s| \exp(i\delta_s)$$

### 3.2 Total reflection at incidence medium/film interface

When the relationships between the refractive indices of the incidence medium, the film and the angle of incidence are such that total internal reflection occurs at the incident medium/film interface the phase dependance on film thickness is different to the characteristic behaviour outlined in Section 3.1.

When total internal reflection occurs at a boundary an evanescent wave exists in the external medium. The electric field strength of this wave decays exponentially with distance from the boundary into the external medium. Frustrated total reflection can occur if there is another material in the region of this evanescent wave causing leakage of energy across this new boundary. The addition of a thin dielectric film onto the boundary does not cause transmission into the external medium and hence total internal

reflection will still occur. If the film is very thin the evanescent wave interacts with the new outer boundary and causes changes in the phase relationships. As the film thickness is increased this interaction decreases until the evanescent wave is effectively contained within the added layer. Figure 12 shows that for zero film thickness the phase difference  $\delta$  and phase changes  $\delta_p$  and  $\delta_s$  are that of the bare substrate. As the film thickness increases these terms change until further increases in film thickness have no additional effect on the phase relationships.

The formulae of Section 3.1 are sufficient to calculate the amplitude reflection coefficients for the total reflection conditions of this section including the effects of film thickness. When  $\sin \phi_2 > 1$  then

$$\cos \phi_2 = -i\sqrt{|1 - \sin^2 \phi_2|}$$

It may be interesting to note that in optical fibre cables the individual optical fibres are clad with low index materials to prevent coupling between fibres and losses from the fibres by physically protecting the inner reflecting interface and the region in which the evanescent wave exists.

### 3.3 Control of phase difference

There are a number of ways of achieving the necessary phase retardation using total internal reflection. An uncoated porro prism of the appropriate refractive index is suitable when a  $90^\circ$  phase retardation is required. Coating of the reflecting surfaces increases the range of achievable phase difference. Completely containing the evanescent wave within the film coating (Section 3.2) is attractive because of the protection from dirt and grease provided to the reflecting surface and the lack of sensitivity of phase difference to film thickness. However, the phase differences obtainable at a fixed angle of incidence are limited by the availability of materials of suitable refractive indices. Figure 12 shows the typical behaviour of the phase terms  $\delta_p$ ,  $\delta_s$  and  $\delta$  as functions of the optical thickness. It can be seen from figure 12 in conjunction with figure 7 that at  $45^\circ$  angle of incidence the maximum phase difference available in this mode must be less than  $90^\circ$  per reflection. Using available materials the achievable range of phase differences is from  $39^\circ$  to  $82^\circ$  (figures 12 and 13).

Coating of the reflecting surfaces with single thin film coatings where total reflection does not occur at the incidence medium/film interface (Section 3.1) provides better control and a wider range of phase difference. Figures 14, 15 and 16 show the range of phase differences that can be achieved using readily available materials. Figures 14 and 15 show the effects of varying the prism index with films of refractive index 1.35 or 2.2 coated on the reflecting surfaces. Figure 16 considers a prism of constant index 1.5 with a variety of film indices. The following points are relevant to figures 14, 15 and 16. In each of these figures the amplitude of oscillation of the phase difference against optical thickness curve depends on the difference between the refractive indices of the prism and the film; larger amplitudes result from larger differences in the indices. The period of oscillation of the curve is not the same for each pair of materials. There are regions near the turning points of the curve where the phase difference remains relatively constant. Multiple solutions of film or optical thickness exist for selected phase differences. In the regions where the phase difference changes slowly with optic path length the phase difference is relatively insensitive to changes in film thickness.

These regions can be considered as near achromatic regions with regard to phase retardation. As the optical pathlength in units of wavelength equals  $nd/\lambda$  it can be seen that the wavelength extent of these near achromatic regions is greater for small optical pathlengths. For example, where a near achromatic region exists over an optical pathlength of 0.25 to 0.5 then this covers a full octave in terms of the wavelength or frequency of light. Wavelengths of 400 to 800 nm could be accommodated with such a condition.

The possible use of multilayer coatings to control phase differences occurring on reflection has been explored previously (ref.10,11). The number of designs to achieve the desired phase difference is increased greatly by the increase of the number of parameters that can be changed i.e. the number and thickness of films of different materials. While computer programmes suitable for use in this type of design problem have been developed in this laboratory a single film solution has been preferred for the wave retardation devices considered here. This approach was selected to limit the number of interfaces between materials, and therefore to decrease the possibility of damaging the coatings with high energy densities.

#### 4. SELECTION OF DESIGN FOR RETROREFLECTIVE WAVEPLATE AT 1.06 $\mu$ m WAVELENGTH

The required function of the porro prism phase retardation device in the laser cavity was to prevent reflected plane polarised electromagnetic radiation from returning through the linear polariser from whence it came until the polarisation state of the beam was changed with a pockells cell. (The practical effect of the pockells cell is to cause an apparent rotation of the linear polariser. Subsequent references to this aspect of operation will refer to rotation of the linear polariser). This function can be achieved by placing a mirror and suitably oriented quarter waveplate in the beam of radiation. The plane of polarisation of the incident beam is set to be at  $45^\circ$  to the privileged directions of the quarter waveplate. The beam passes through the quarter waveplate, is reflected from the mirror, through the quarter waveplate again and back to the linear polariser. The phase difference introduced between the resolved orthogonal vectors of the beam results in an effective  $90^\circ$  rotation of the plane of polarisation and hence the return beam is unable to pass through the linear polariser (figure 17). When the linear polariser is rotated so that the plane of polarisation of the beam is parallel to one of the privileged directions of the quarter waveplate no rotation of the plane of polarisation occurs in the waveplate mirror combination and the beam is returned to and passes through the linear polariser.

The porro prism has advantages over the mirror, quarter waveplate combination. It is easier to align and small misalignment in the horizontal plane can be tolerated. Also, one side of the incident beam is translated by the double reflection within the prism and some desirable averaging of the beam energy within the cavity occurs. When the beam from the linear polariser is plane polarised at an angle of  $45^\circ$  to the line of intersection of the two reflecting faces (the vertex of the prism) and there is  $0^\circ$  phase difference per reflection in the prism there is an effective rotation of the plane of polarisation of the return beam and the return beam is not passed by the linear polariser (figure 18). When the linear polariser is rotated so that the plane of polarisation is either normal or parallel to the vertex of the prism the return beam is transmitted by the linear polariser.

It can be seen from figure 19 that with a  $90^\circ$  phase difference per reflection in the prism there is no effective rotation of the plane of polarisation of the return beam. For this prism to function as required it needs to be preceded by a quarter waveplate as was the case with the plane mirror. The arrangement

of quarter waveplate and porro prism retains the alignment and averaging advantages over the mirror, quarter waveplate solution.

#### 4.1 Selected design of prism with $0^\circ$ phase difference per reflection

To achieve a  $0^\circ$  phase difference per reflection a coating of magnesium fluoride, optical thickness  $0.75\lambda$  and refractive index of 1.38 at  $1.06 \mu\text{m}$  on a prism of refractive index 1.79 at  $1.06 \mu\text{m}$  is required as shown by figure 20. The critical angle of the prism is  $34^\circ$ , (figure 21) and so the maximum total misalignment and divergence allowed before transmission of the beam through the reflecting surface of the prism occurs is  $11^\circ$ . The effects of  $2^\circ$  of misalignment are shown in figure 22 where the phase difference per reflection for angles of incidence of  $43^\circ$ ,  $45^\circ$  and  $47^\circ$  are plotted for this combination of film thickness and index, and prism index. From the geometry of the Porro prism an increase in one angle of incidence results in a corresponding decrease in the other. The total effect of misalignment on the phase difference through the prism is then the sum of the effects on phase at the two relevant angles of incidence. The change of phase difference with change of angle of incidence is not symmetric about the nominal angle of incidence of  $45^\circ$ .

Reference to figure 15 shows that a  $0^\circ$  phase difference per reflection occurs with the combination of a film of refractive index 2.2 on a prism of index 1.45. From figure 21 the critical angle for the prism material in air is  $45.6^\circ$ . This means that the total misalignment and divergence allowed before transmission occurs through the reflecting surface is  $1.4^\circ$ . The effect of a  $1^\circ$  misalignment is shown in figure 23 where the phase difference per reflection is plotted for angles of incidence of  $44^\circ$ ,  $45^\circ$  and  $46^\circ$ .

#### 4.2 Selected design of prism with $90^\circ$ phase difference per reflection

While this prism has to be used with a quarter waveplate to meet the requirement given in Section 4, it is included as a practical alternative solution.

A  $90^\circ$  phase difference per reflection can be achieved by using a thin film coating of titanium dioxide, optical thickness  $0.11\lambda$  and refractive index 2.2 at  $1.06 \mu\text{m}$ , on a prism of refractive index 1.5 at  $1.06 \mu\text{m}$  (figure 16). The critical angle of the prism is  $41.8^\circ$  (figure 21) allowing a total misalignment and divergence of  $3^\circ$  before the total internal reflection condition is exceeded and transmission of the beam occurs through the surface of the prism. The effects of  $2^\circ$  of misalignment are shown in figure 24 where the phase difference per reflection for angles of incidence of  $43^\circ$ ,  $45^\circ$  and  $47^\circ$  are plotted.

### 5. EVALUATION OF COATED PRISMS

Two porro prisms were coated with thin films of magnesium fluoride and titanium dioxide. The resultant phase relationships of a beam of light through each prism were measured to test the validity of the calculated characteristics.

#### 5.1 Method of measurement

Plane polarised light was incident on the prism with the electric vector inclined at an angle of  $45^\circ$  to the vertex of the prism (figure 25). The reflected beam from the prism passed through a polariser (analyser) and the relative intensity of the beam was measured with an SGD 100 silicon diode detector. The analyser was mounted so that the plane of transmission of the electric vector was either parallel with, or perpendicular to, the plane of the electric vector of the incident beam.

### 3.2 Measurement of phase difference

The light reflected from the prism is, in general, elliptically polarised. The measured intensities can be simply related to the phase difference between the s and p components of light from the prism(ref.12).

Consider the orthogonal directions x and y where the direction of x is parallel with the vertex of the prism and x and y are perpendicular to the direction of propagation of the beam. The general equation of the path of the resultant vector for elliptically polarised light is

$$\frac{x^2}{a_1^2} + \frac{y^2}{a_2^2} - \frac{2xy (\cos \delta)}{a_1 a_2} - \sin^2 \delta = 0$$

where  $a_1$  and  $a_2$  are the vector component amplitudes in the x and y directions

and  $\delta$  is the phase difference between the components in the x and y direction; (ref.13).

Because the beam is totally internally reflected within the prism and the resolved vectors of the input beam in the x and y direction are of equal amplitude  $a_1 = a_2$  in the output beam. Setting  $a_1 = a_2 = 1$  the general equation is simplified to

$$x^2 + y^2 - 2xy (\cos \delta) - \sin^2 \delta = 0$$

Because  $a_1 = a_2$  the major and minor axes of the ellipse are inclined at  $45^\circ$  to the x and y axes. Rotating the axes through an angle  $\phi = 45^\circ$ , the rotated axes are w and v;

$$w = x \cos \phi - y \sin \phi$$

$$v = x \cos \phi + y \sin \phi$$

and the equation becomes

$$w^2 (1 - \cos \delta) + v^2 (1 + \cos \delta) = \sin^2 \delta$$

$$\text{ie } w^2 \left( \frac{1 - \cos \delta}{\sin^2 \delta} \right) + v^2 \left( \frac{1 + \cos \delta}{\sin^2 \delta} \right) = 1$$

This is the equation of an ellipse with major and minor axes of

$$a = \sqrt{\frac{\sin^2 \delta}{1 - \cos \delta}}$$

$$b = \sqrt{\frac{\sin^2 \delta}{1 + \cos \delta}}$$

where a and b are the amplitudes of component vectors along the w and v axes. It can be shown that

$$\cos \delta = \frac{a^2 - b^2}{a^2 + b^2}$$

ie

$$\cos \delta = \frac{I_w - I_v}{I_w + I_v}$$

where  $I_w$  and  $I_v$  are the intensities of the component beams in the w and v directions.

### 5.3 Prism coated with magnesium fluoride

The prism design to give  $0^\circ$  phase difference per reflection (Section 4.1) was based on the use of glass with a refractive index of 1.79 at  $1.06 \mu\text{m}$ . A prism was made from glass with refractive index of 1.76 and coated with magnesium fluoride. The lower index glass was used for the prism because it was readily available. The phase characteristics of this glass coated with magnesium fluoride have been calculated and graphed in figure 26. The minimum phase difference per reflection for these materials is about  $4^\circ$  when the optical film thickness is  $0.65\lambda$  at  $1.06 \mu\text{m}$ . Spectral reflectance measurements of the two coated surfaces indicate that the actual optical film thickness was  $0.653\lambda$  at  $1.06 \mu\text{m}$ .

The measured signals representing the values of  $I_w$  and  $I_v$  for this prism were 0.1 v and 8.6 v giving a phase difference of  $12.2^\circ$  for the prism ( $6.1^\circ$  per reflection) and an extinction ratio  $I_w/I_v$  of 1:86.

### 5.4 Prism coated with titanium dioxide

The design of paragraph 4.2 was used when making the second prism for evaluation. Subsequent to the coating of the prism it was found that the index of the glass was actually 1.45 at  $1.06 \mu\text{m}$ . Spectral reflectance measurements of the two coated surfaces indicate that the film thicknesses were  $0.241\lambda$  @  $1.06 \mu\text{m}$  and  $0.251\lambda$  @  $1.06 \mu\text{m}$ . Figure 27 shows the calculated phase characteristics of the prism and from this data the expected phase difference is  $72^\circ$  per reflection or  $144^\circ$  for the prism.

The measured signals for  $I_w$  and  $I_v$  were 7.2v and 1.35v giving a phase difference of  $133^\circ$  for the prism ( $66.5^\circ$  per reflection) and an extinction ratio  $I_w/I_v$  of 5.3:1.

### 5.5 Discussion of results

The results for the prism coated with magnesium fluoride are in good agreement with the design calculations. It is reasonable to assume that a zero or near zero phase change per reflection would have been achieved if a higher index glass had been available.

The original objective of a  $90^\circ$  phase difference per reflection at  $1.06 \mu\text{m}$  was not achieved with the prism coated with titanium dioxide because glass of the required refractive index was not used. The measured phase difference agrees quite well with the calculated values when the calculations are based on the



materials and film thicknesses used. It is considered that the results from each prism confirm the correctness of the calculations and also the fact that these devices can be made.

#### 6. CONCLUSION

It is possible to design and make retroreflective waveplates using a single film coating on each reflecting surface of a porro prism. The most important of the waveplates are the zero, quarter, and half waveplate and each of these can be made using readily available materials. The data in this report can be used to design phase retardation devices of different configurations where special reflecting waveplates are required.

The reflecting waveplate has particular application in those infrared spectral regions where no useful birefringent materials are available.

## NOTATION

$\theta_i$	angle of incidence
$a$	amplitude of vector component
$b$	amplitude of vector component
$d$	physical thickness of film
$i$	$\sqrt{-1}$
$n$	refractive index
$p, s$	subscripts specifying polarisation of electromagnetic wave
$r$	amplitude reflection coefficients
$v, w$	orthogonal axes
$x, y$	orthogonal axes
$\delta, \delta_s, \delta_p$	phase angles
$\delta_z$	phase thickness of film
$\theta$	angle of rotation of axes
$\phi$	angle of incidence or refraction
$\lambda$	wavelength

REFERENCES

No.	Author	Title
1	Jenkins, F.A. and White, H.E.	"Fundamentals of Optics". Third Edition, p.515 (McGraw Hill Book Company, New York, 1957)
2	Bennett, J.M. and Bennett, H.E.	"Polarization". Handbook of Optics, W.G. Driscoll editor (McGraw Hill Book Company, New York, 1978)
3	Bennett, J.M.	"A Critical Evaluation of Rhomb-type Quarter Wave Retarders". Applied Optics, Vol.9, No.9, p.2123, September 1970
4	Heavens, O.S.	"Optical Properties of Thin Solid Films". (London, Butterworths Scientific Publications, 1955)
5	Berning, P.H.	"Theory and Calculations of Optical Thin Films". Physics of Thin Films, Vol.1 (New York, Academic Press, 1963)
6	Heavens, O.S.	"Optical Properties of Thin Films". Progress in Physics, Vol.23 (London, The Physical Society, 1960)
7	Weinstein, W.	"Computations in Thin Film Optics". Vacuum, Vol.IV, No.1, January 1954
8	Venning, J.R.	"The Spectral Characteristics of Metal Film Beam-Splitters". ERL-0123-TR, January 1980
9	Vasicek, A.	"Optics of Thin Films". (Amsterdam, North Holland Publishing Company, 1960)
10	Kard, P.G.	"On the Influence of Thin Films on Total Reflection". Optics and Spectroscopy, Vol.VI, No.4, p.339, April 1959
11	Mauer, P.	"Phase Compensation of Total Internal Reflection". Journal of the Optical Society of America Vol.56, No.9, p.1219, September 1966
12	Richards, J.	Private Communication, March 1981
13	Jenkins, F.A. and White, H.E.	"Fundamentals of Optics". Third Edition, p.227 (McGraw Hill Book Company, New York, 1957)

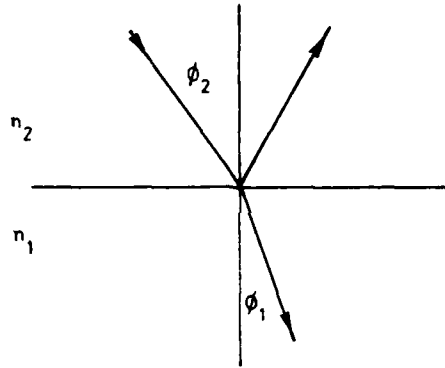
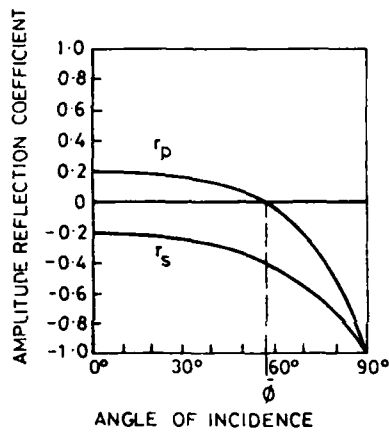
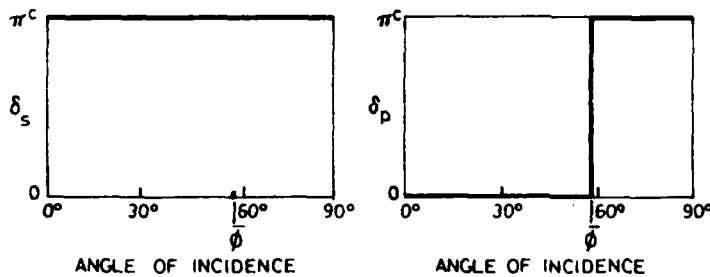


Figure 1. Single surface reflection



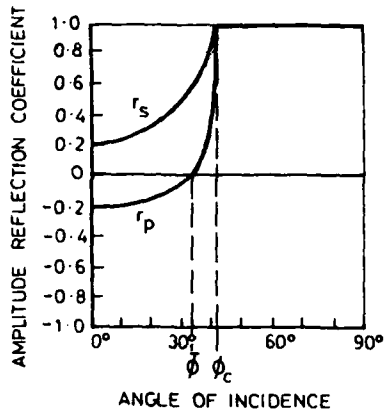
$\bar{\phi}$  is Brewster angle  
 Incident medium  $n_2=1.0$   
 Reflecting material  $n_1=1.5$

Figure 2. Amplitude reflection coefficients as a function of angle of incidence ( $n_1 > n_2$ )



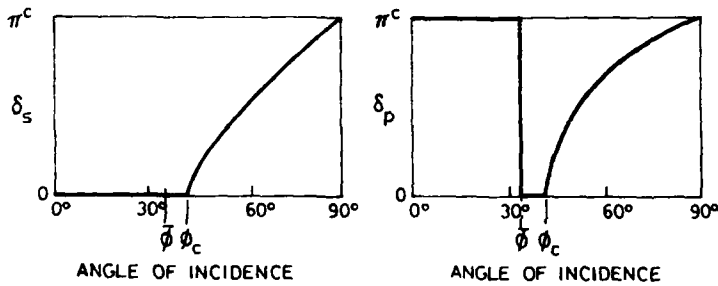
$\bar{\phi}$  is Brewster angle  
 Incident medium  $n_2=1.0$   
 Reflecting material  $n_1=1.5$

Figure 3. Phase change on reflection as a function of angle of incidence ( $n_1 > n_2$ )



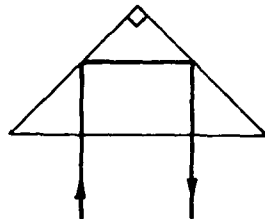
$\bar{\phi}$  is Brewster angle  
 $\phi_c$  is Critical angle  
 Incident medium  $n_2=1.5$   
 External medium  $n_1=1.0$

Figure 4. Amplitude reflection coefficients as a function of angle of incidence ( $n_1 < n_2$ )



$\bar{\phi}$  is Brewster angle  
 $\phi_c$  is Critical angle  
 Incident medium  $n_2=1.5$   
 External medium  $n_1=1.0$

Figure 5. Phase change on reflection as a function of angle of incidence ( $n_1 < n_2$ )



Prism  $n > 1.414$   
 External medium  $n=1.0$

Figure 6. Porro Prism

At  $45^\circ$  angle of incidence  $\delta_p = 2\delta_s$  and  $\delta = \delta_s$   
External medium  $n=1$

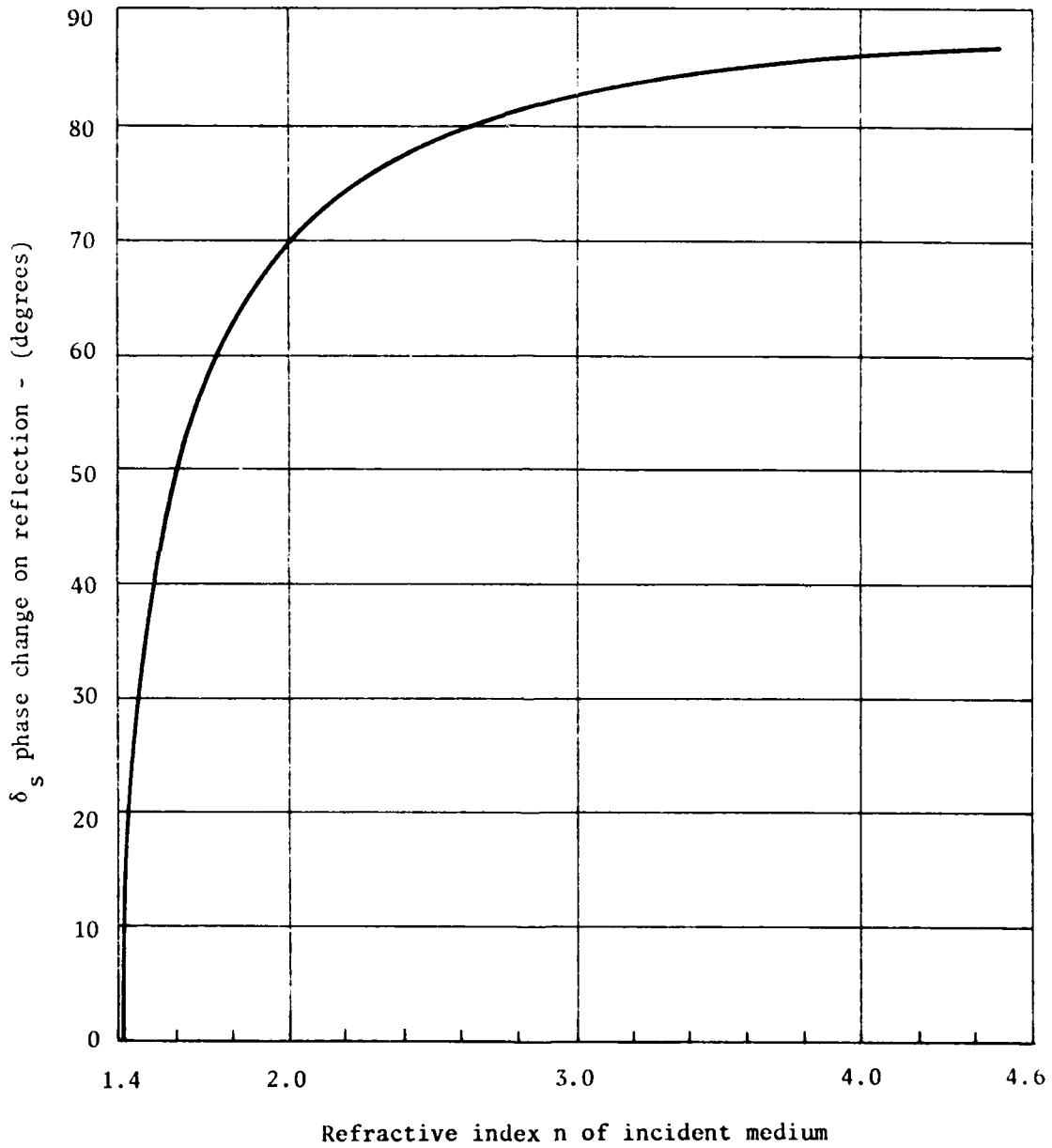


Figure 7. Phase change on reflection at  $45^\circ$  angle of incidence as a function of refractive index

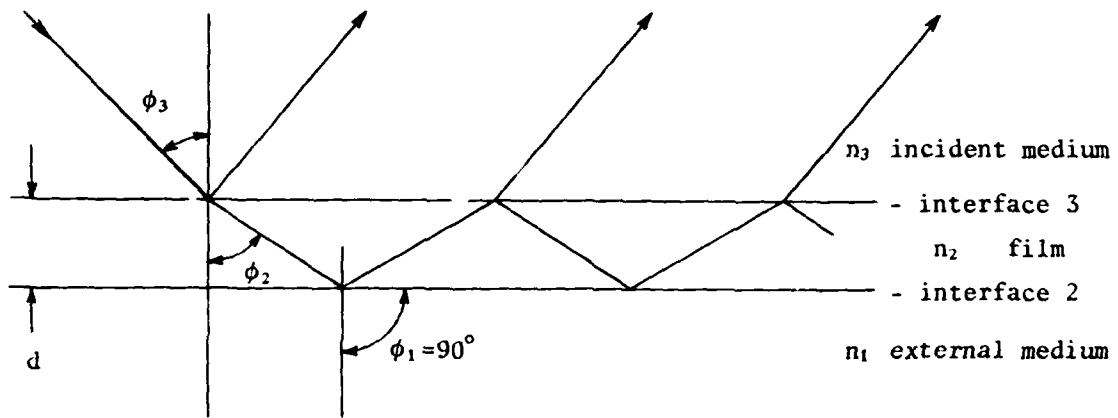


Figure 8. Total reflection from a coated surface

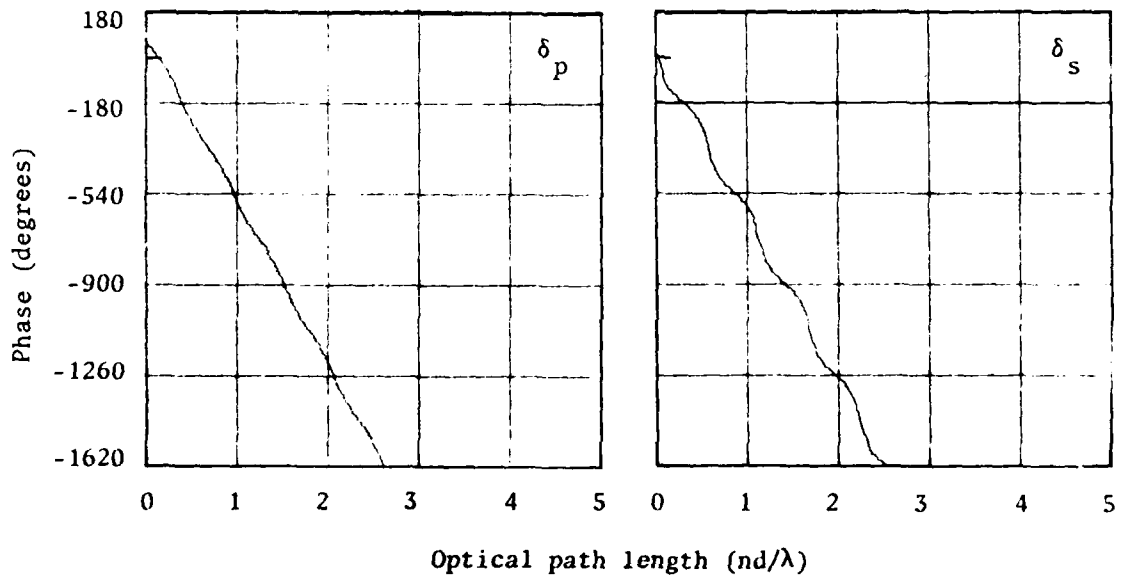
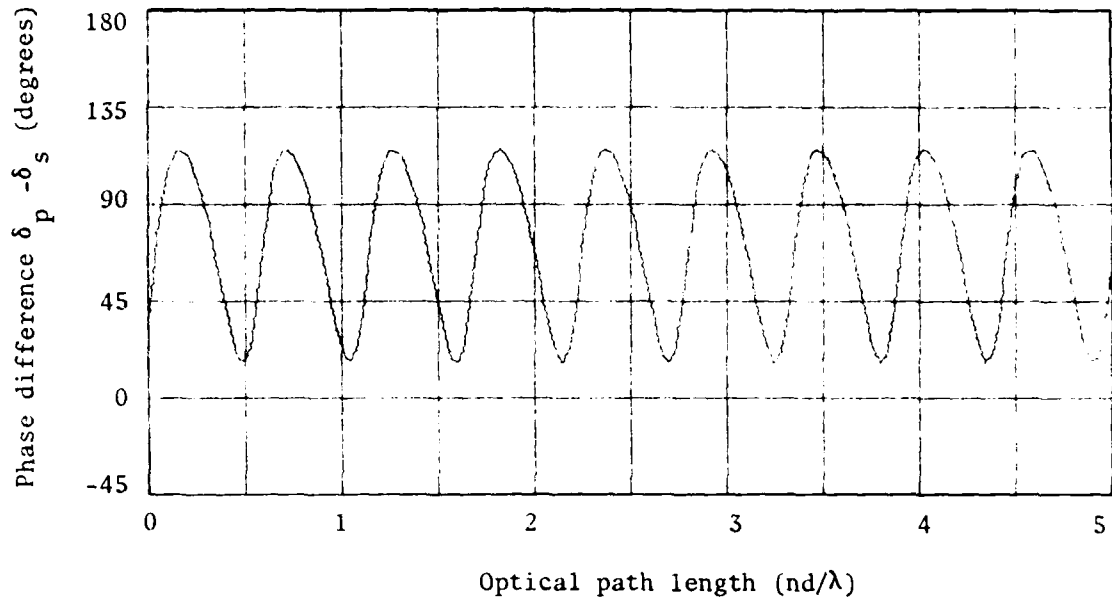


Figure 9. Phase angles for  $n_2 = 2.5$ ,  $n_3 = 1.5$ ,  $AI = 45^\circ$



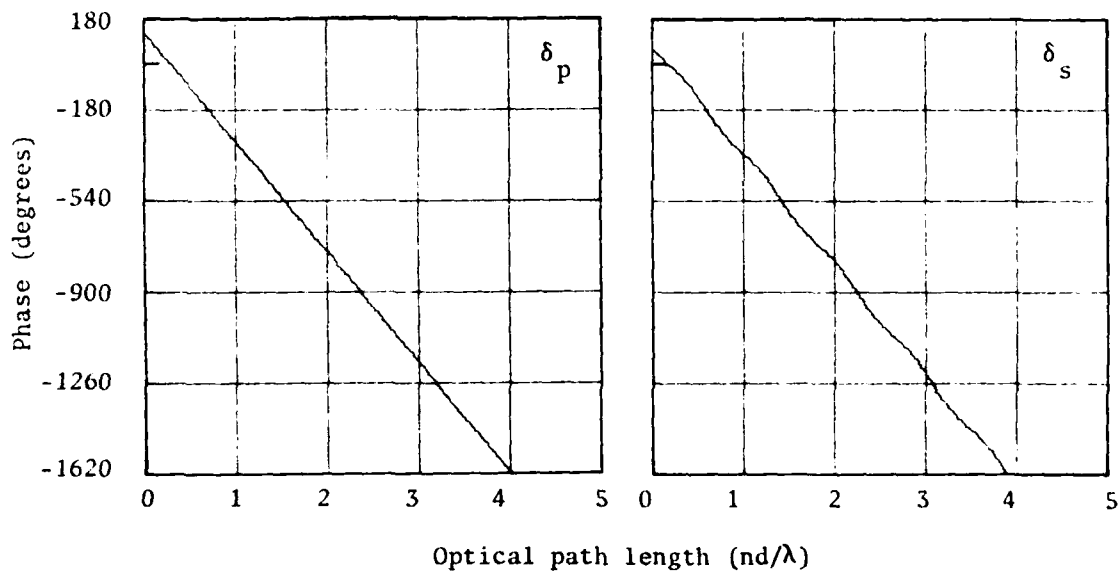
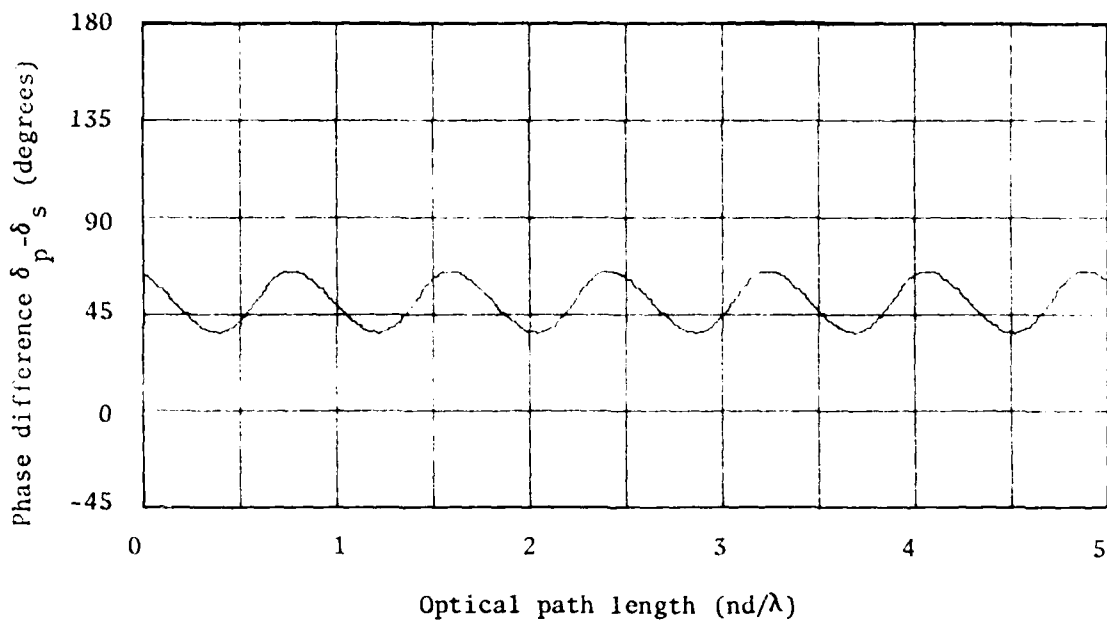


Figure 10. Phase angles for  $n_2 = 1.6$ ,  $n_3 = 1.8$ ,  $A_1 = 45^\circ$

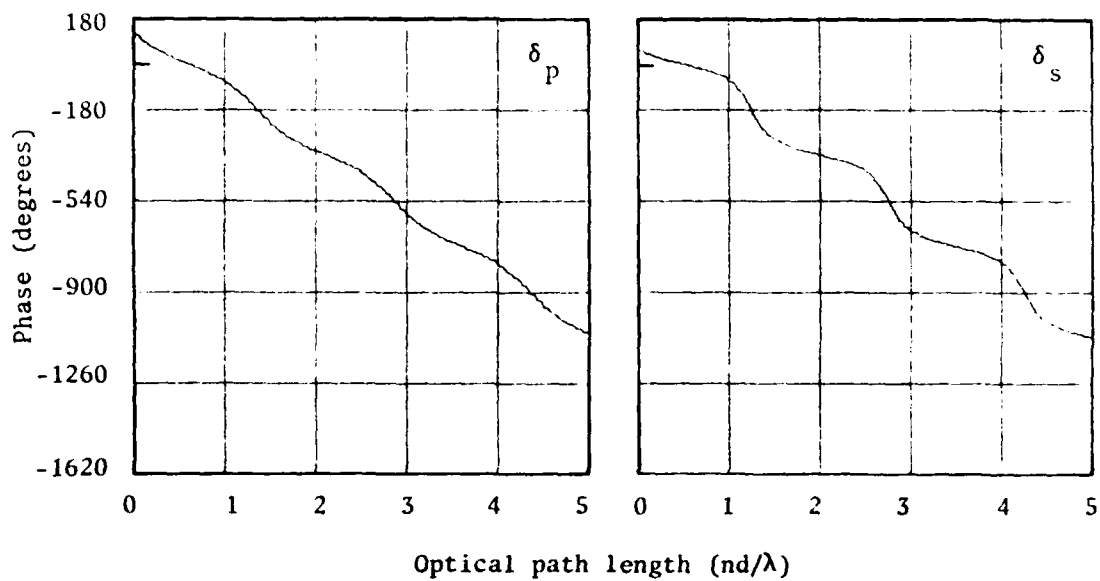
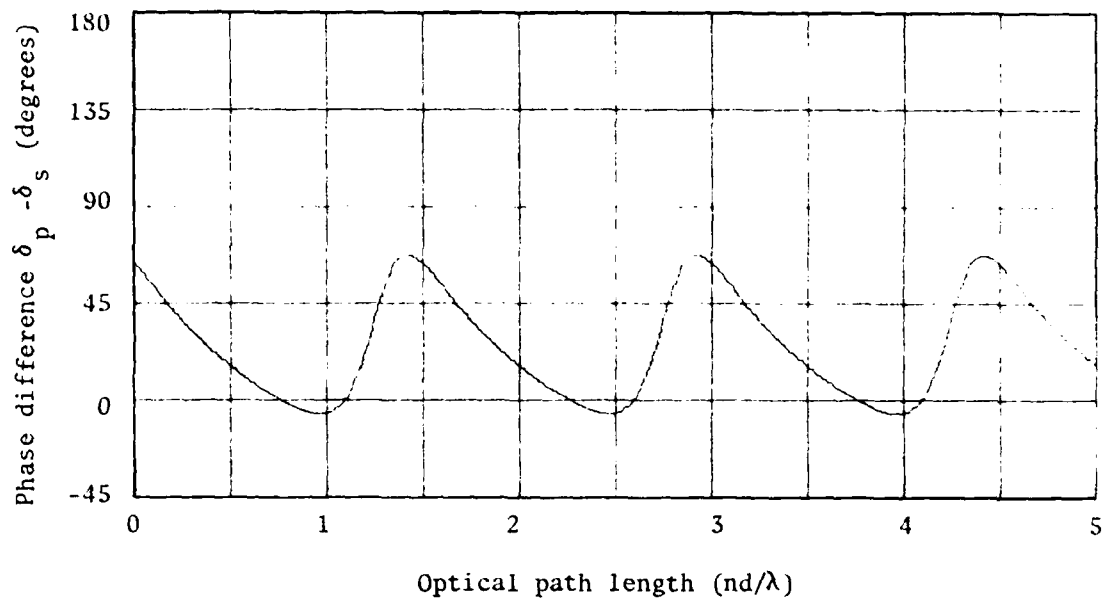


Figure 11. Phase angles for  $n_2 = 1.35$ ,  $n_3 = 1.8$ ,  $AI = 45^\circ$

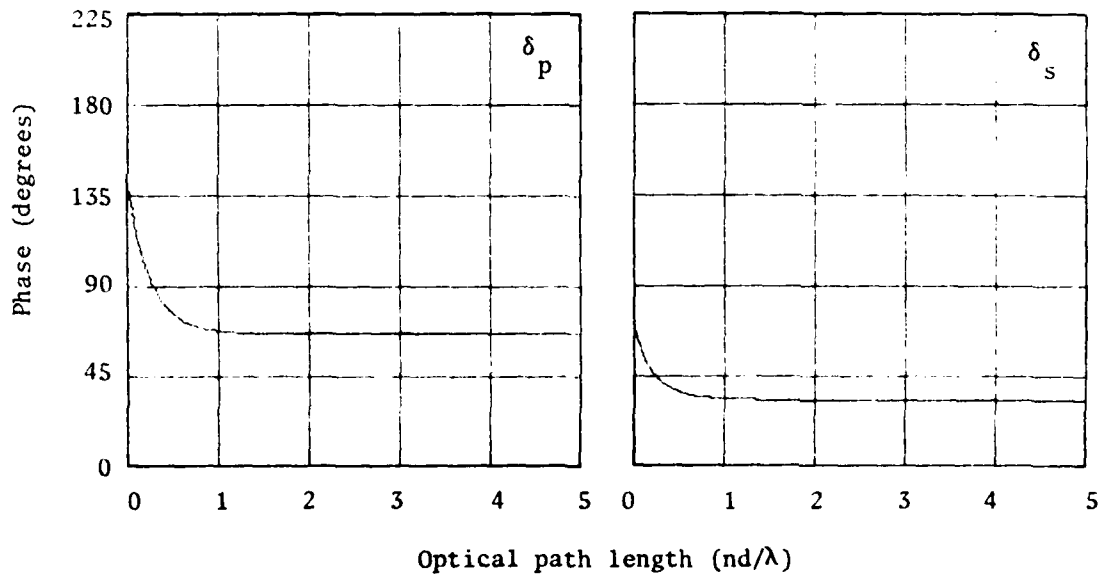
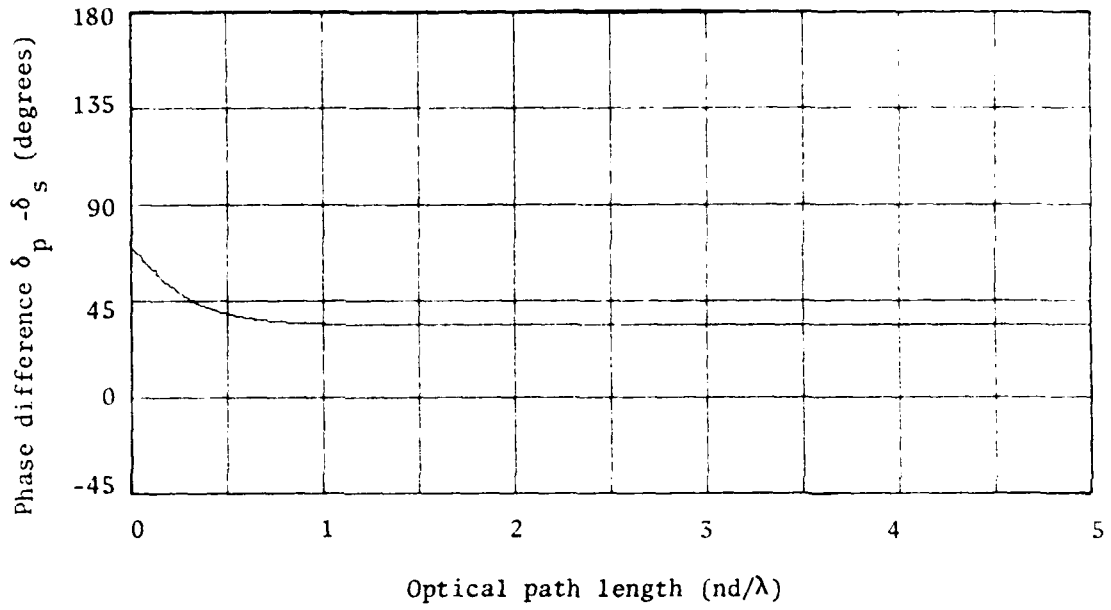


Figure 12. Phase angles for  $n_2 = 1.35$ ,  $n_3 = 2.0$ ,  $AI = 45^\circ$

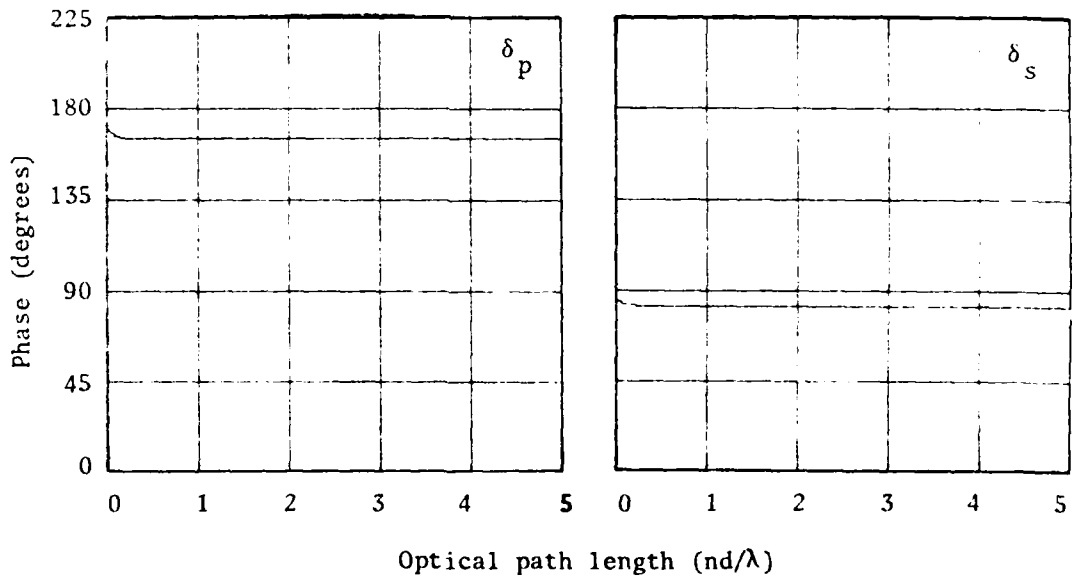
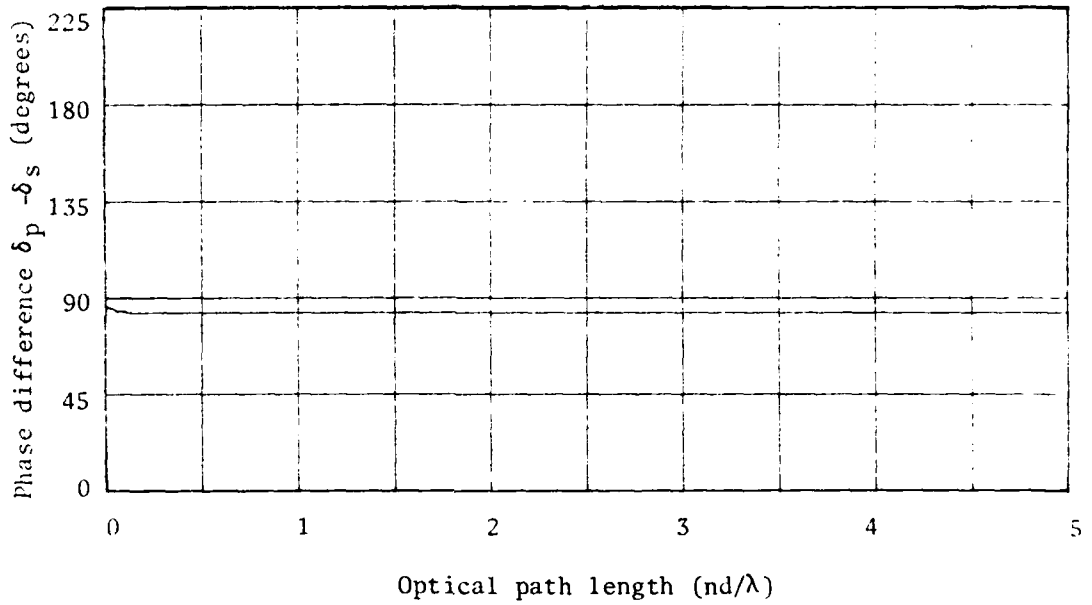


Figure 13. Phase angles for  $n_2 = 1.35$ ,  $n_3 = 4.0$ ,  $AI = 45^\circ$

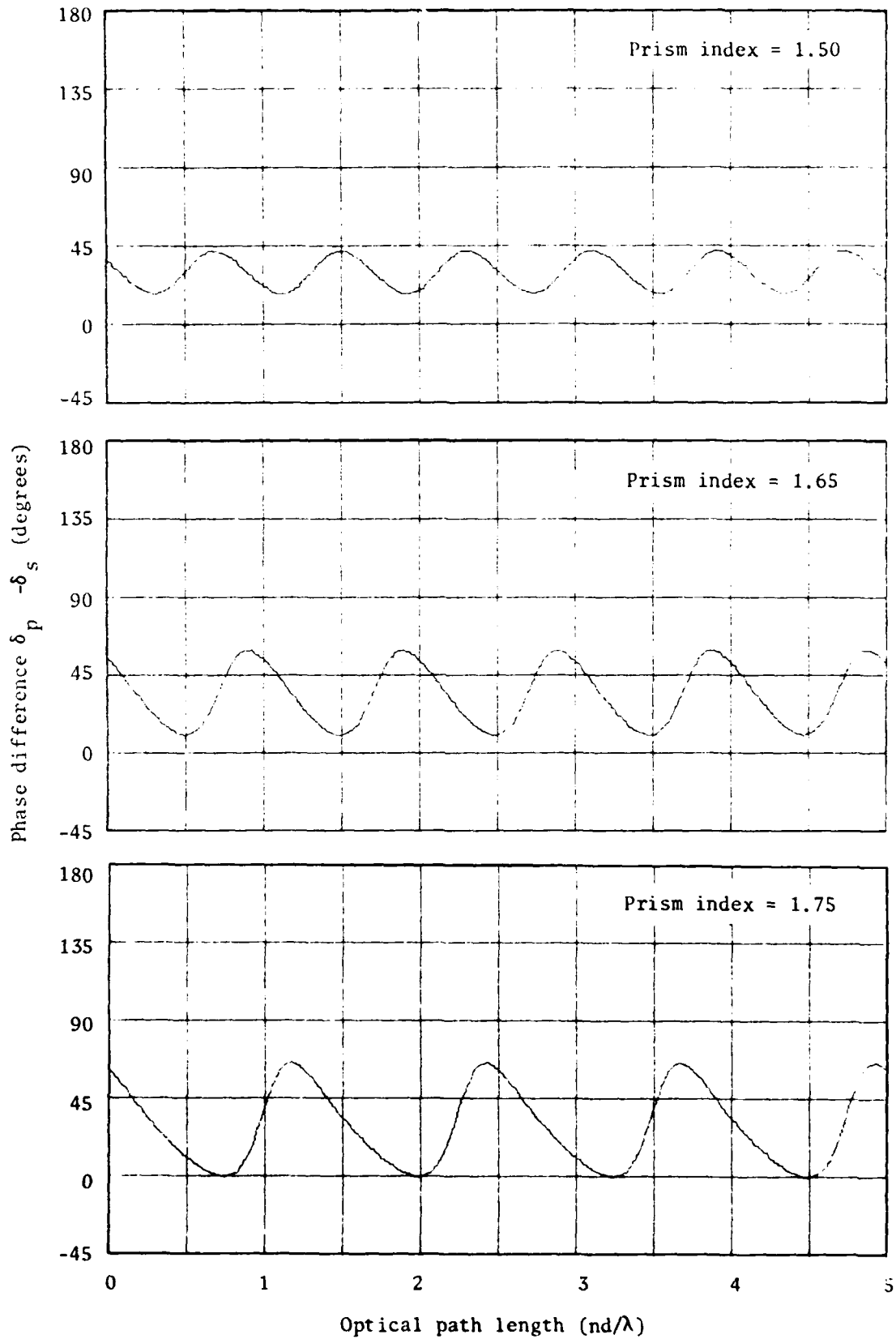


Figure 14. Variation of phase difference with variation of prism index; film index = 1.35, angle of incidence =  $45^\circ$

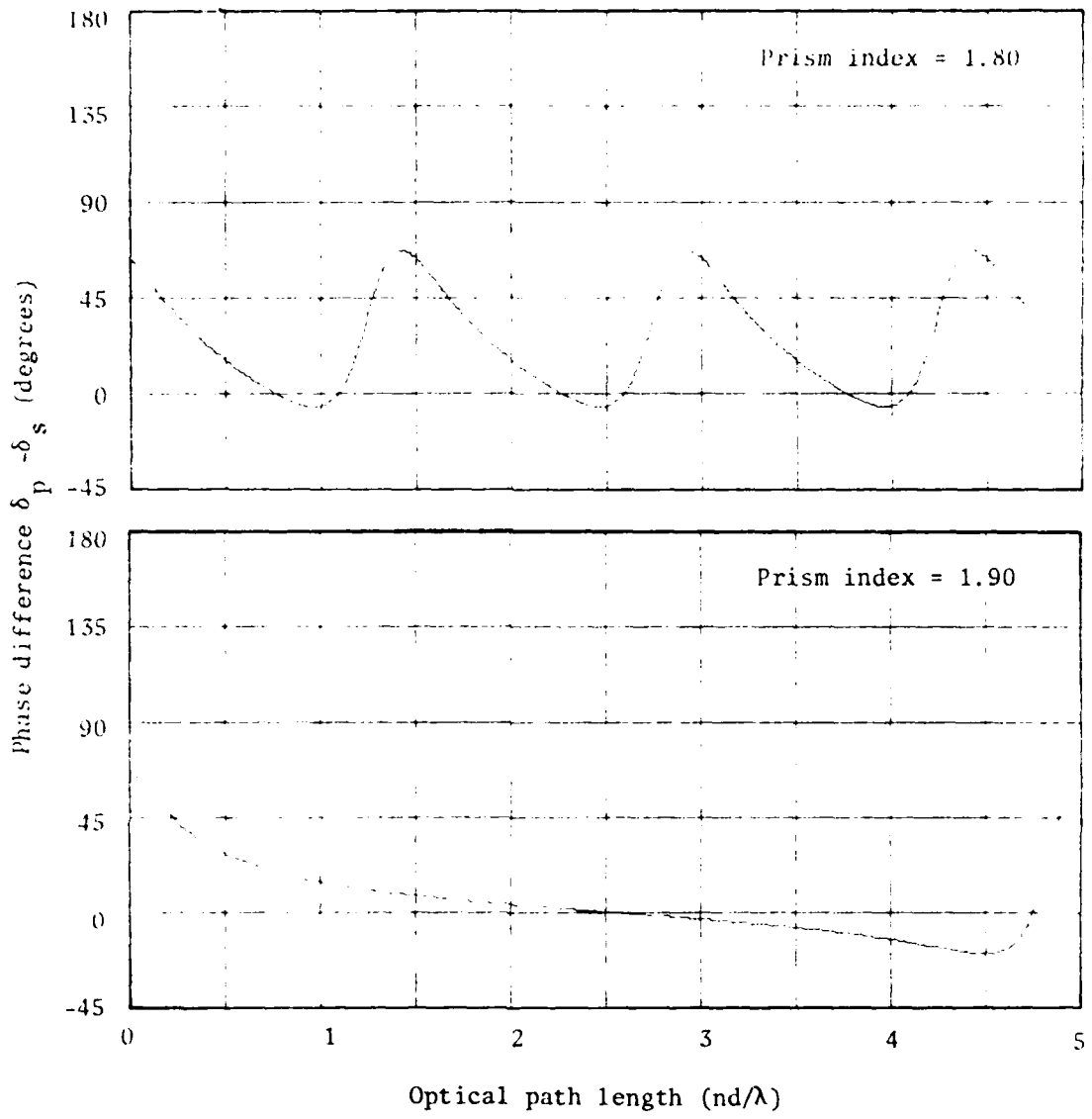


Figure 14(Contd.).

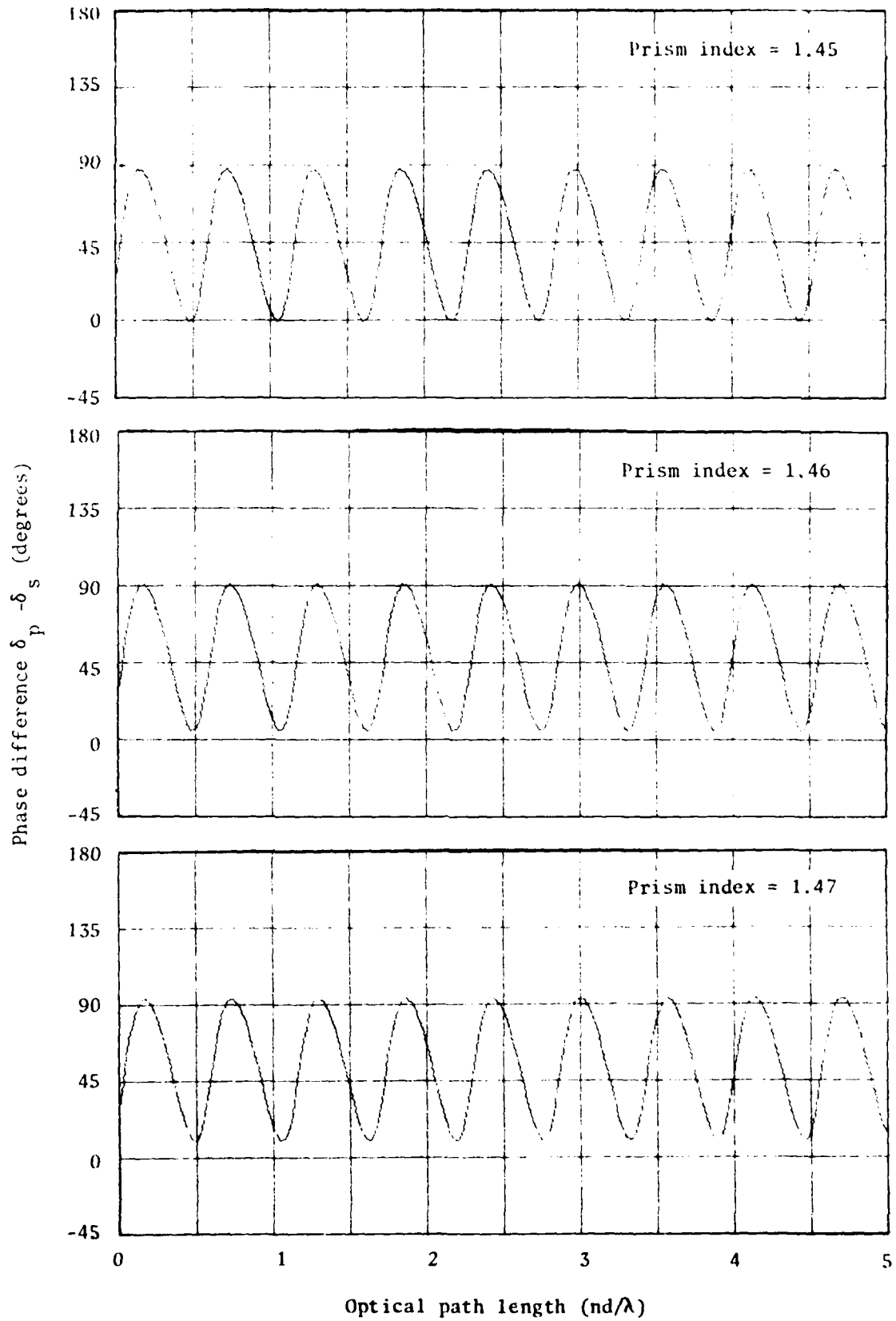


Figure 15. Variation of phase difference with variation of prism index; film index = 2.2, angle of incidence =  $45^\circ$

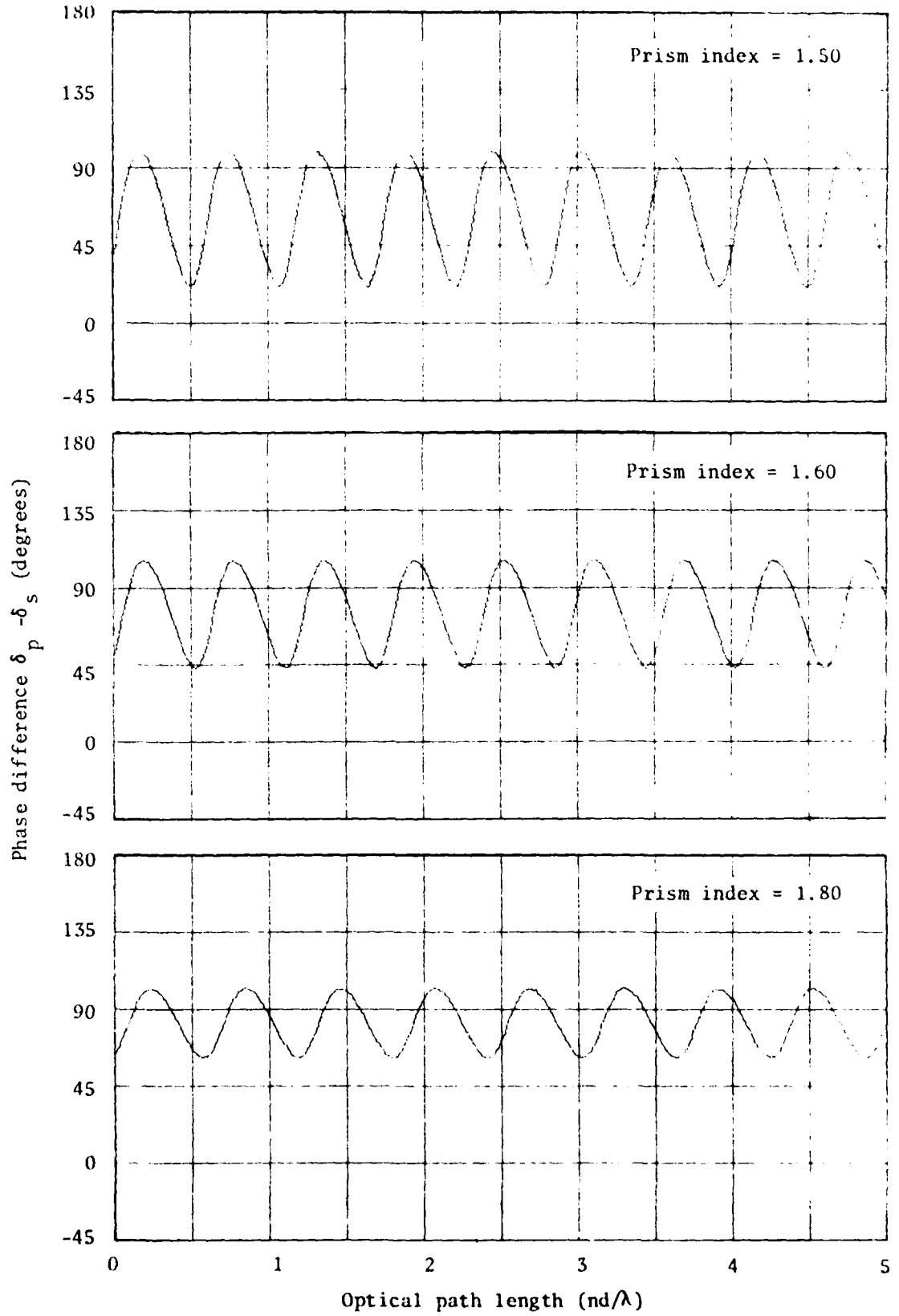


Figure 15(Contd.).



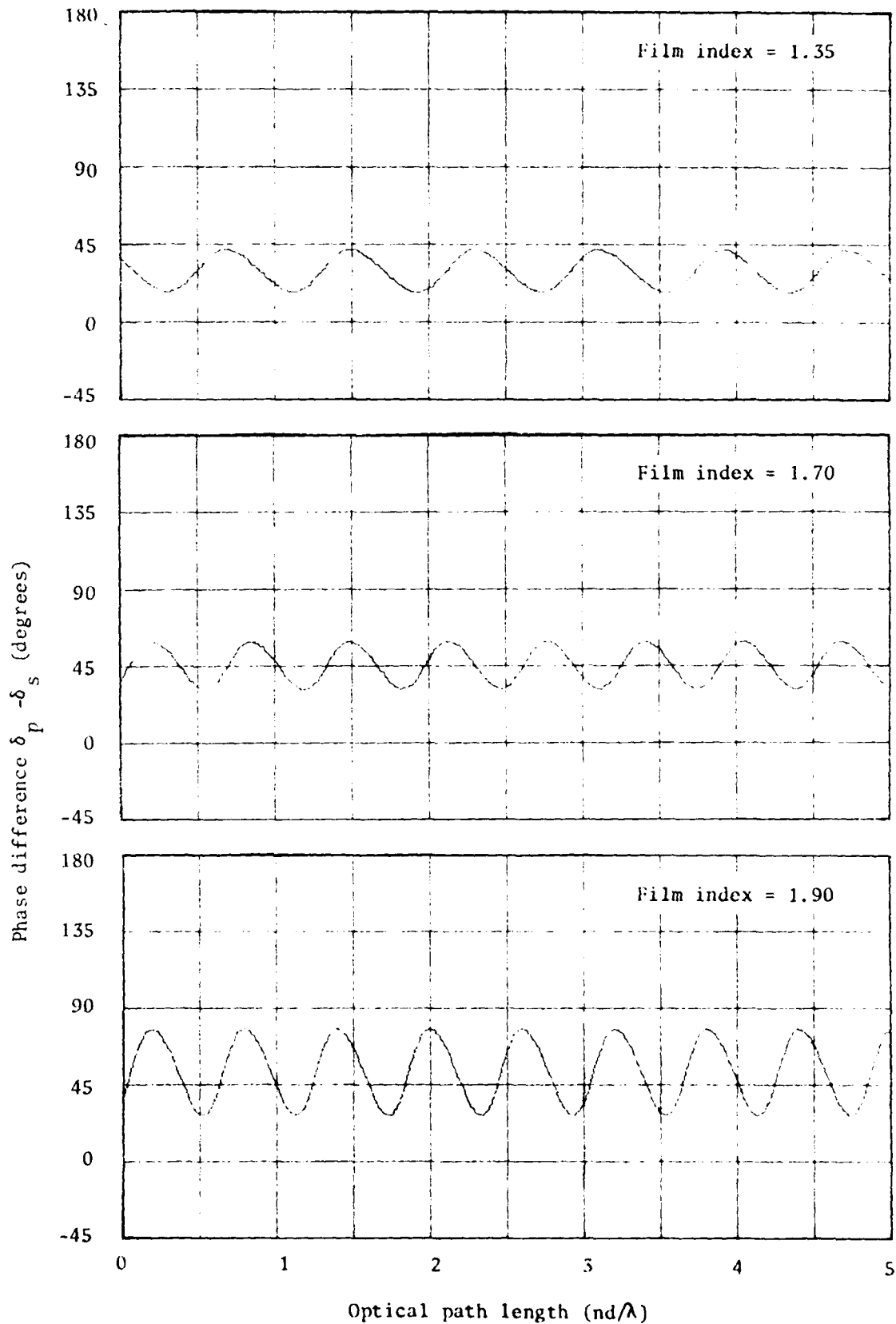


Figure 16. Variation of phase difference with variation of film index; prism index = 1.5, angle of incidence =  $45^\circ$

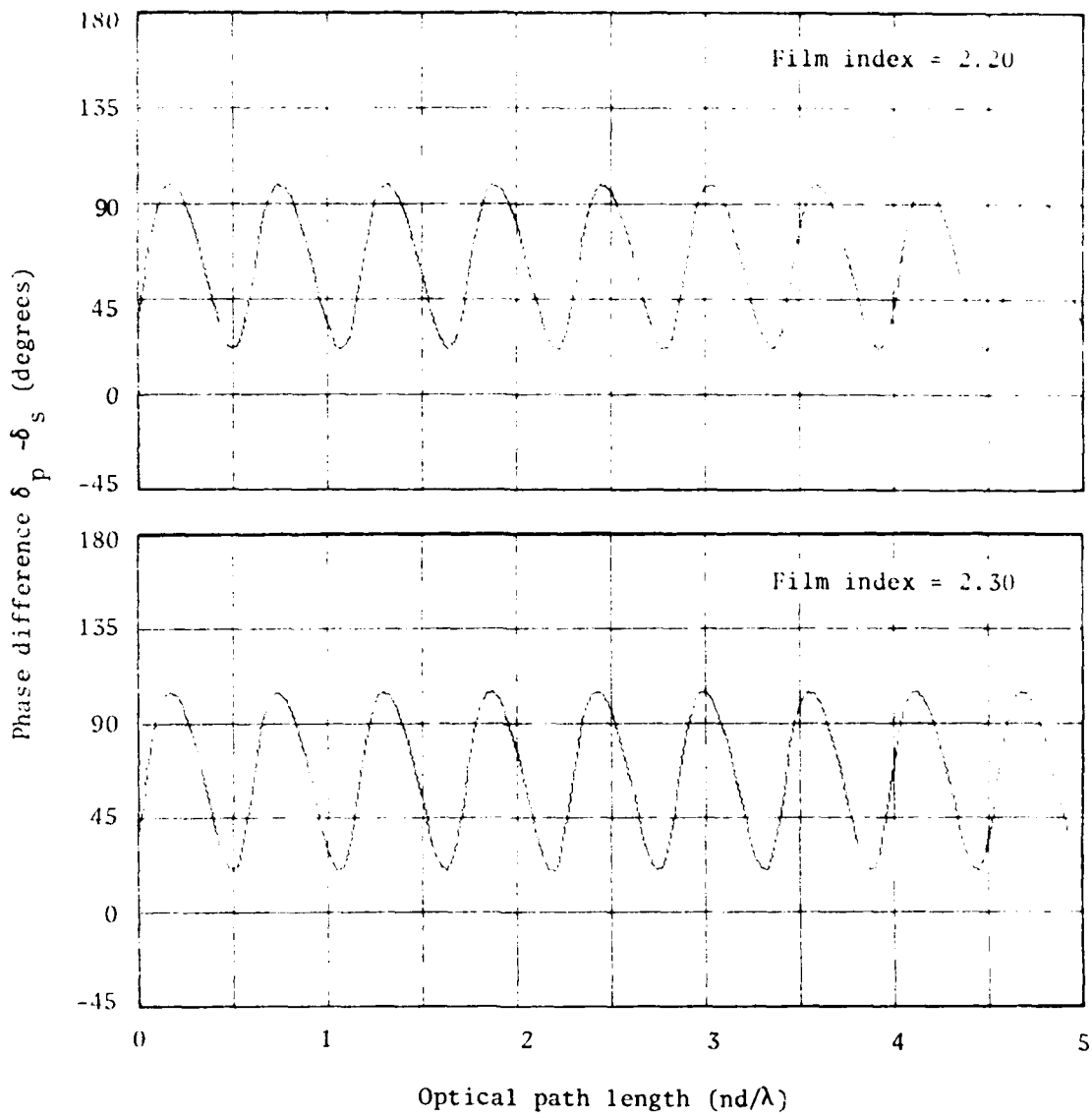


Figure 16(Contd.).

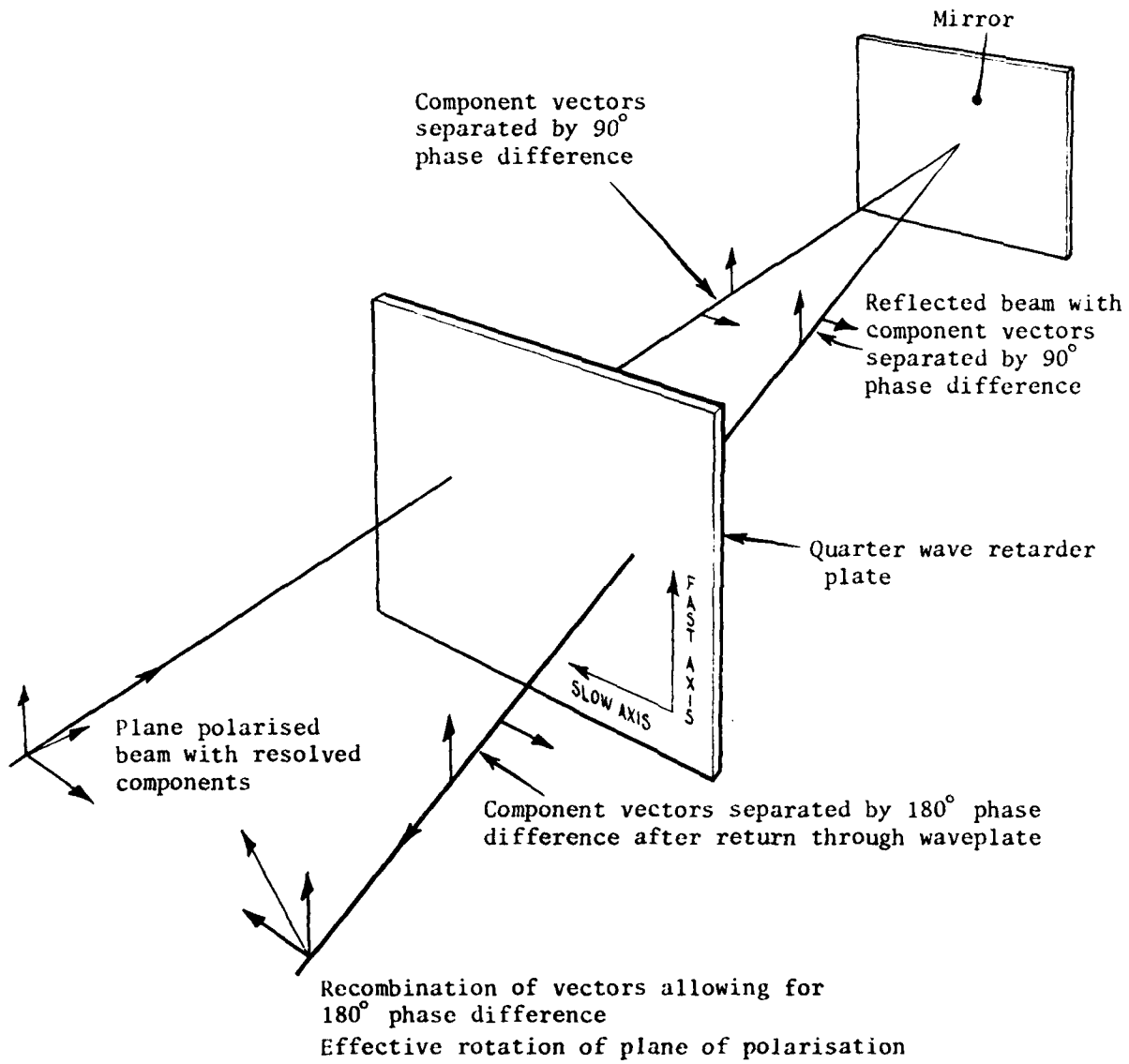


Figure 17. Retroreflective mirror and quarter wave plate retarder

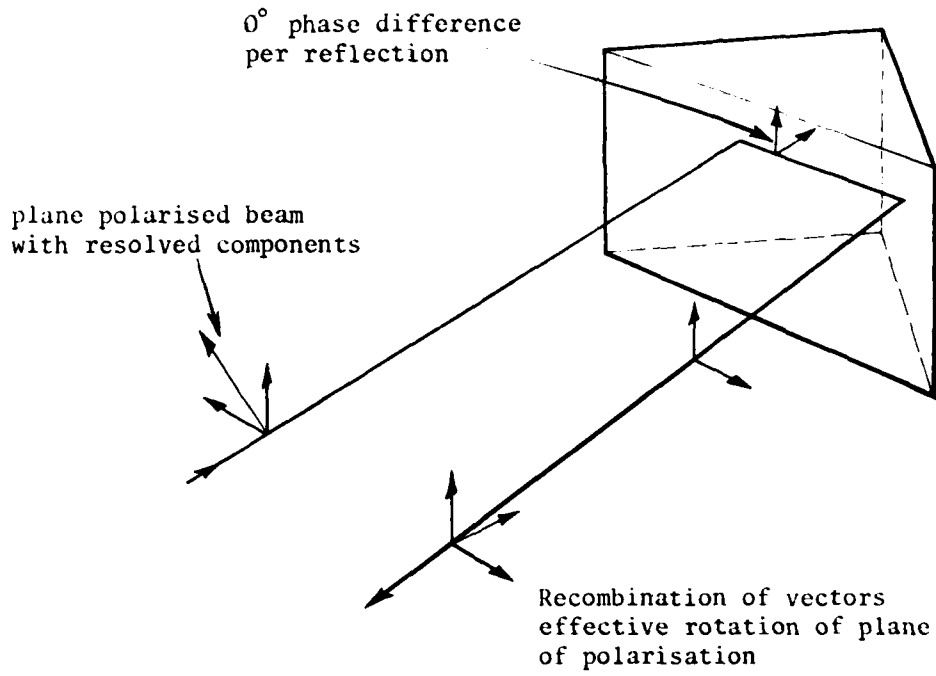


Figure 18. Retroreflecting porro prism retarder; 0° phase difference per reflection

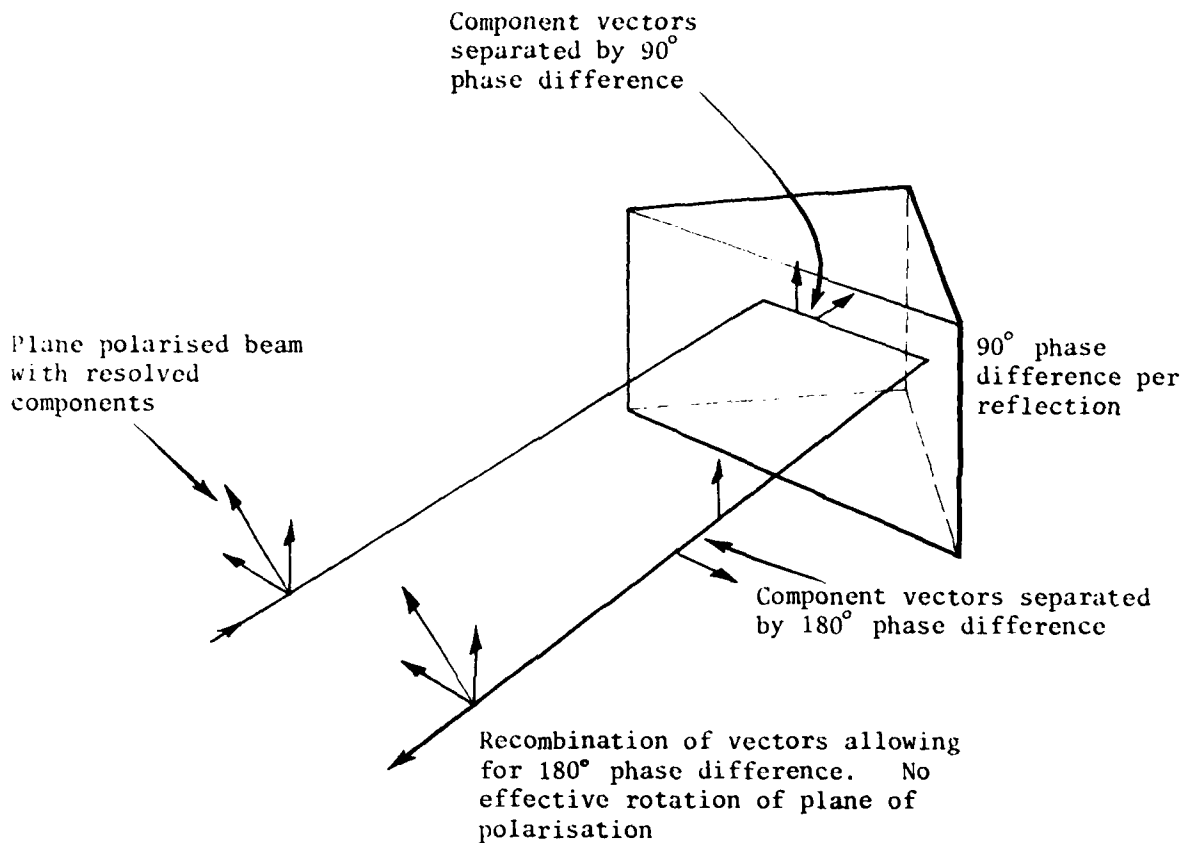


Figure 19. Retroreflecting porro prism retarder;  $90^\circ$  phase difference per reflection

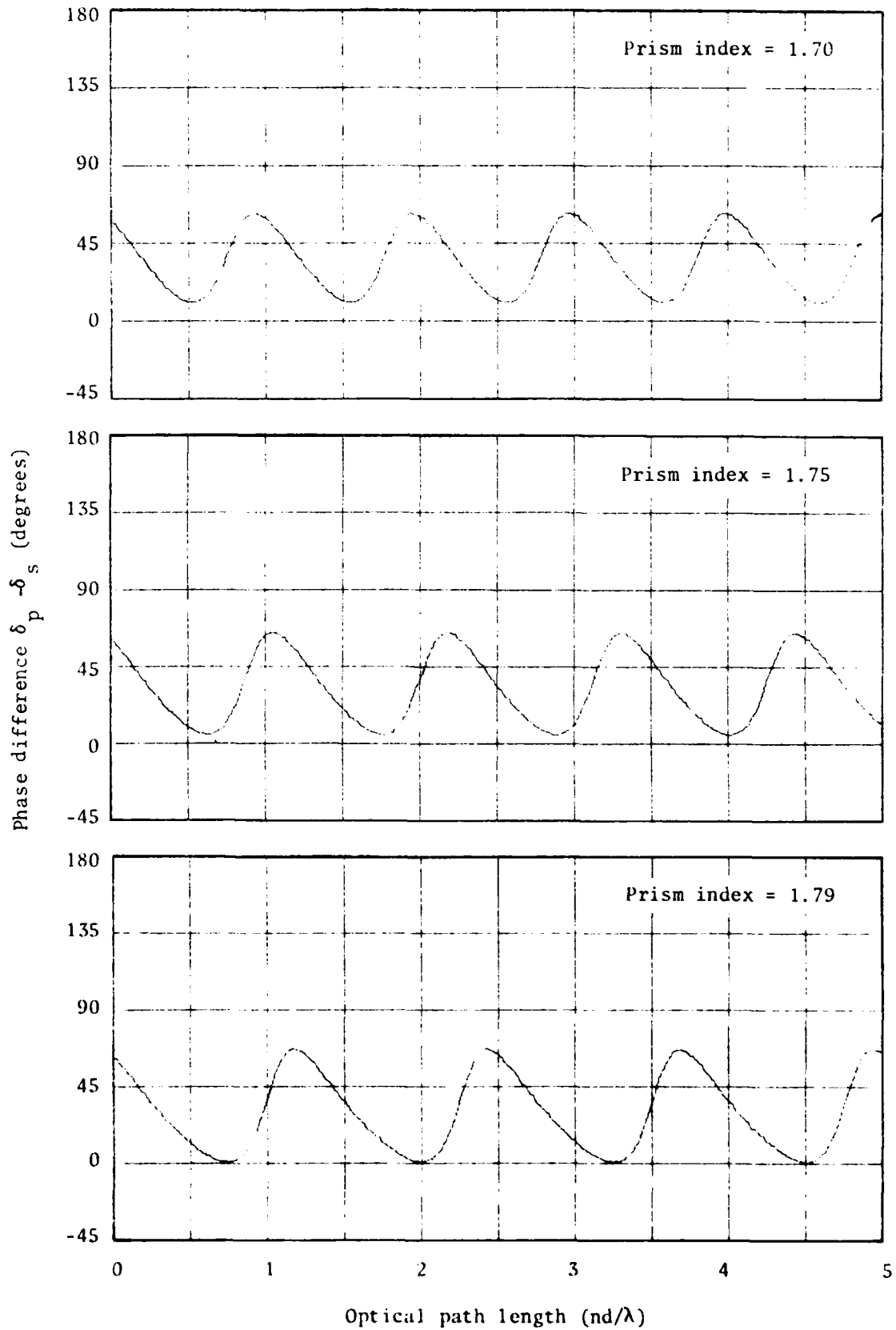


Figure 20. Variation of phase difference with variation of prism index; film index = 1.38, angle of incidence = 45

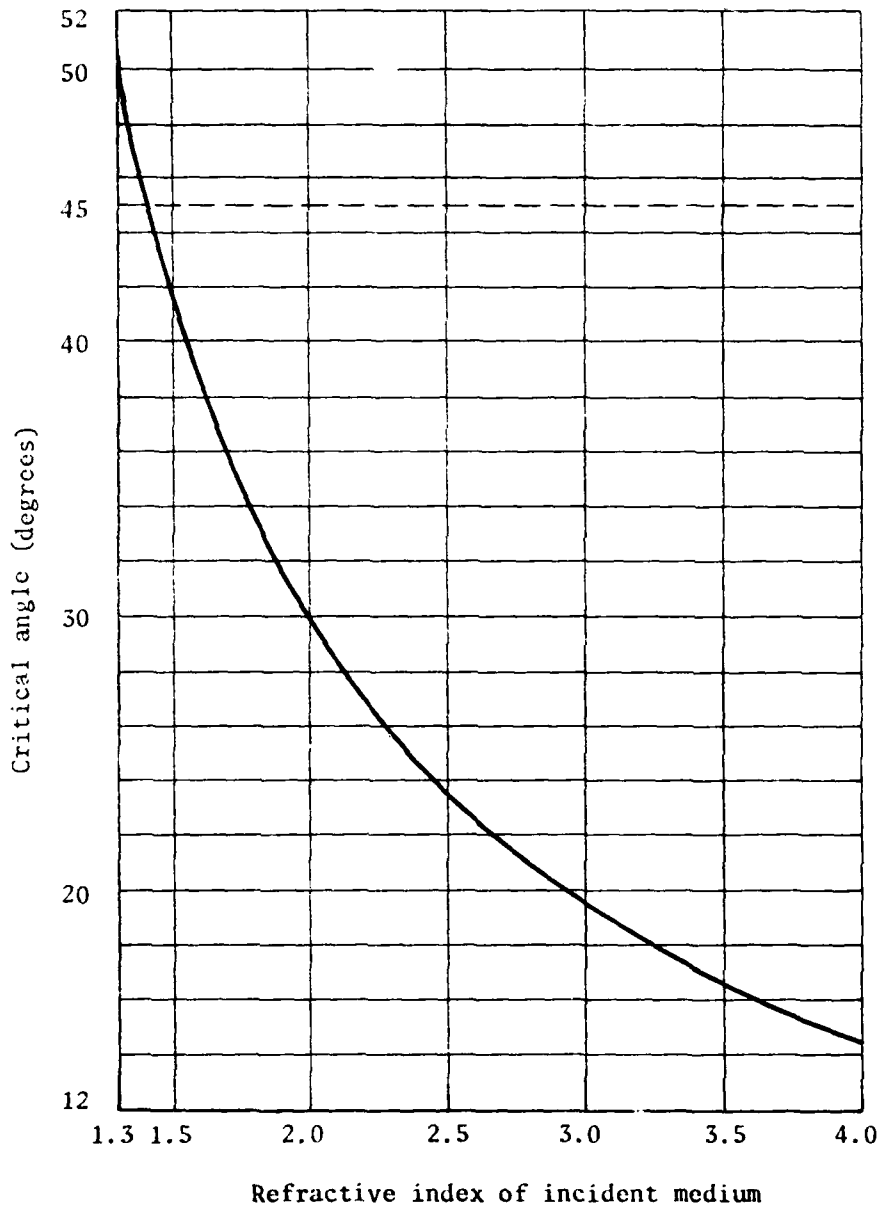


Figure 21. Critical angle of materials in air

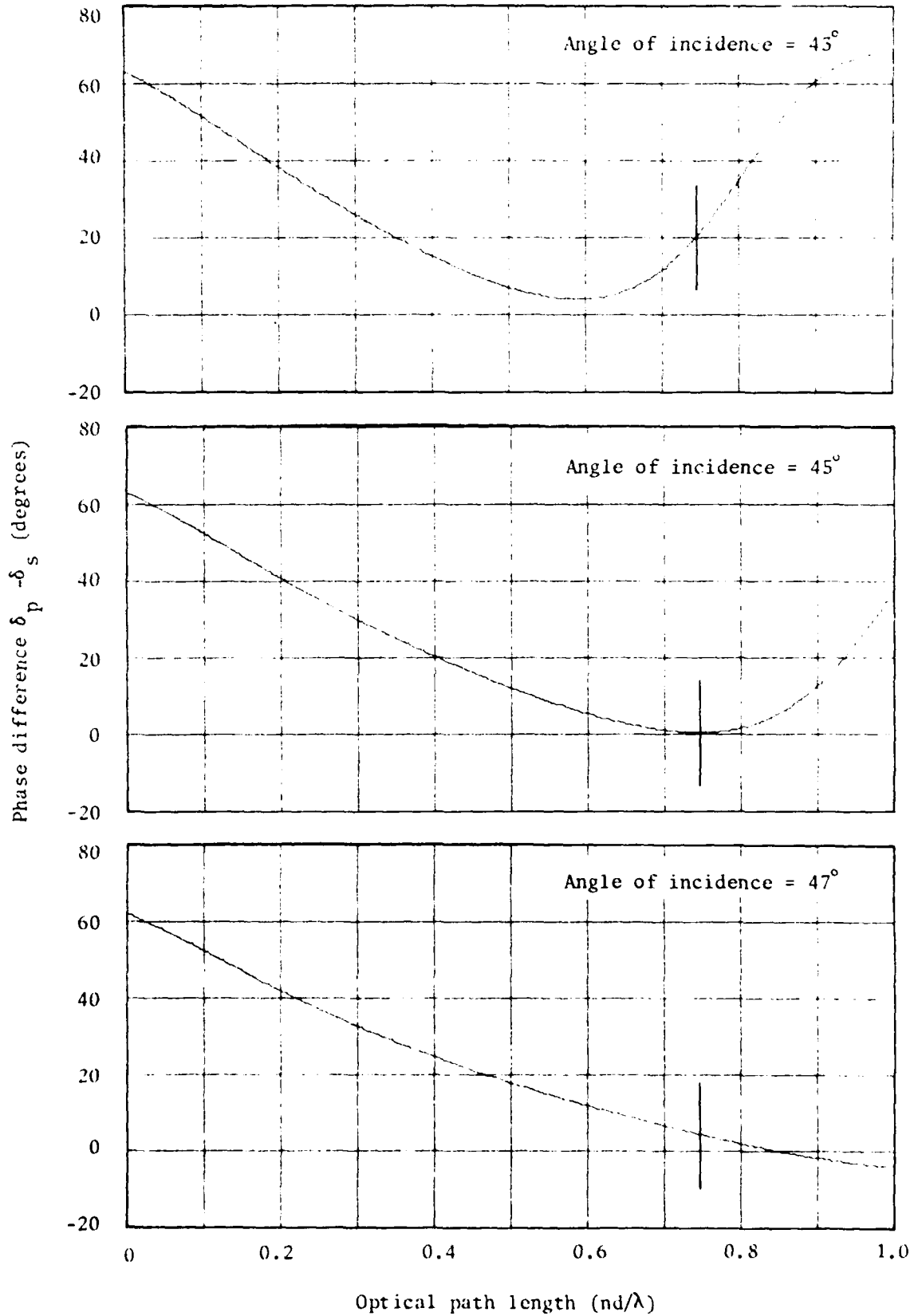


Figure 22. Variation of phase difference with variation of angle of incidence; prism index = 1.79, film index = 1.38



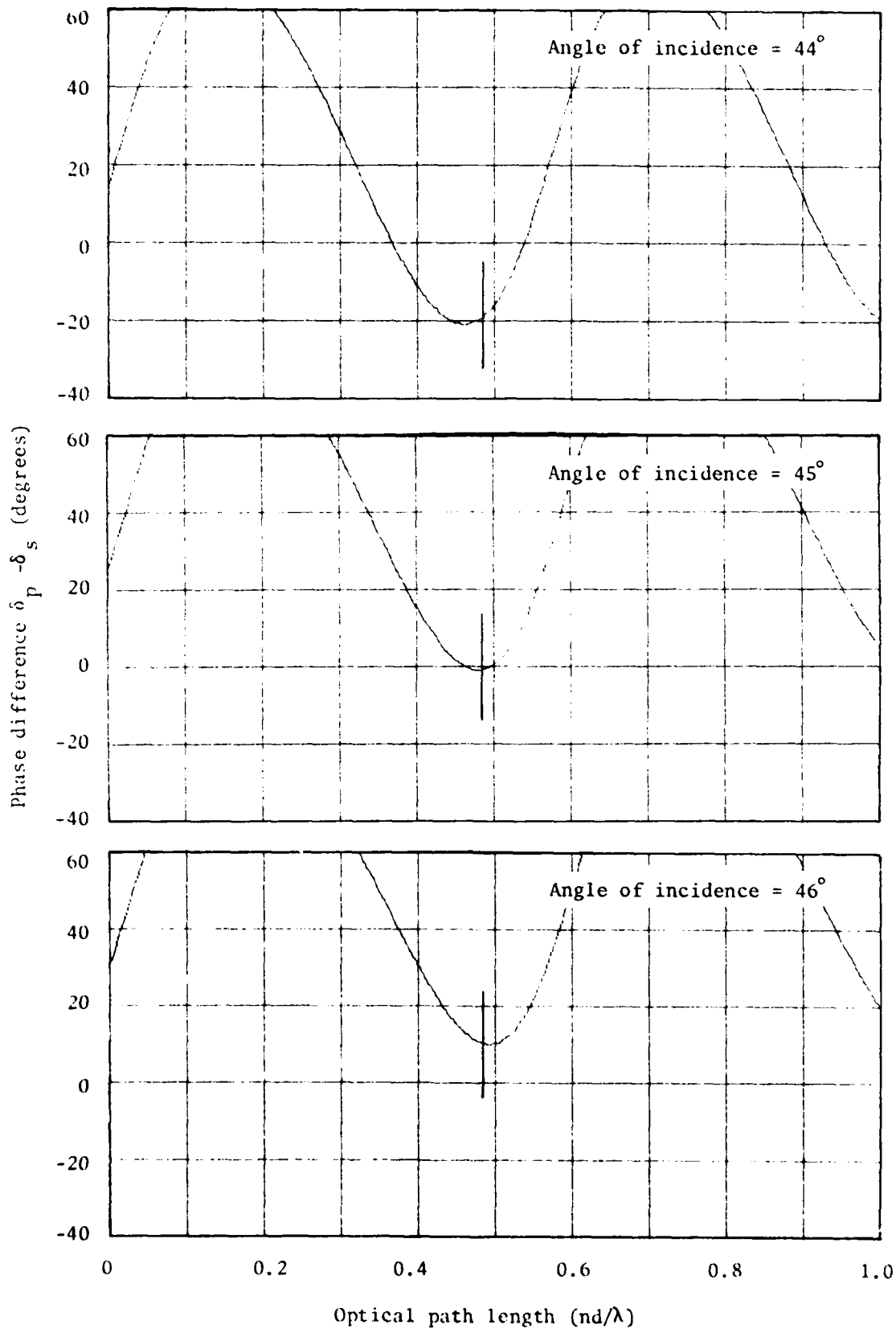


Figure 23. Variation of phase difference with variation of angle of incidence; prism index = 1.45, film index = 2.20

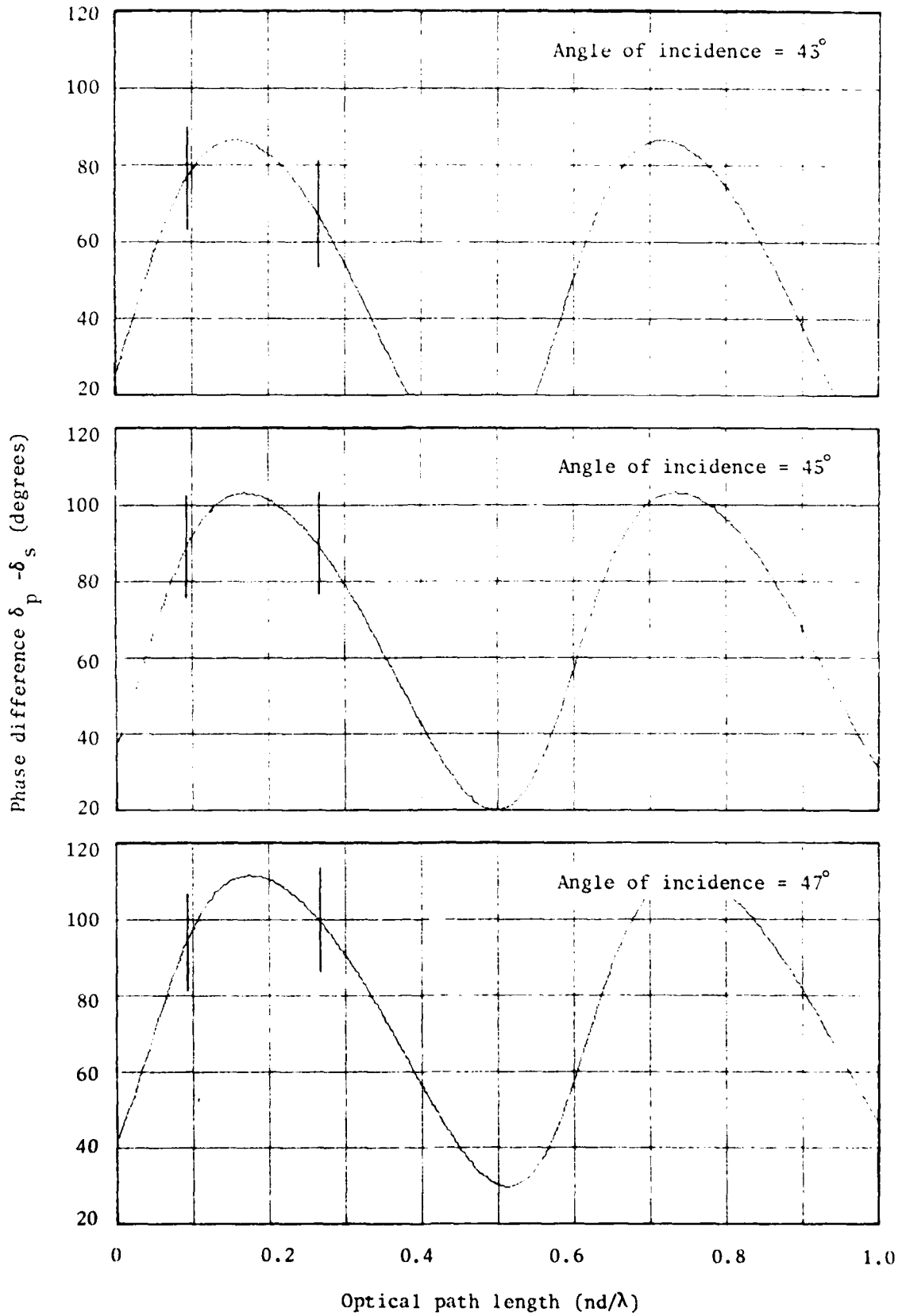


Figure 24. Variation of phase difference with variation of angle of incidence; prism index = 1.50, film index = 2.27

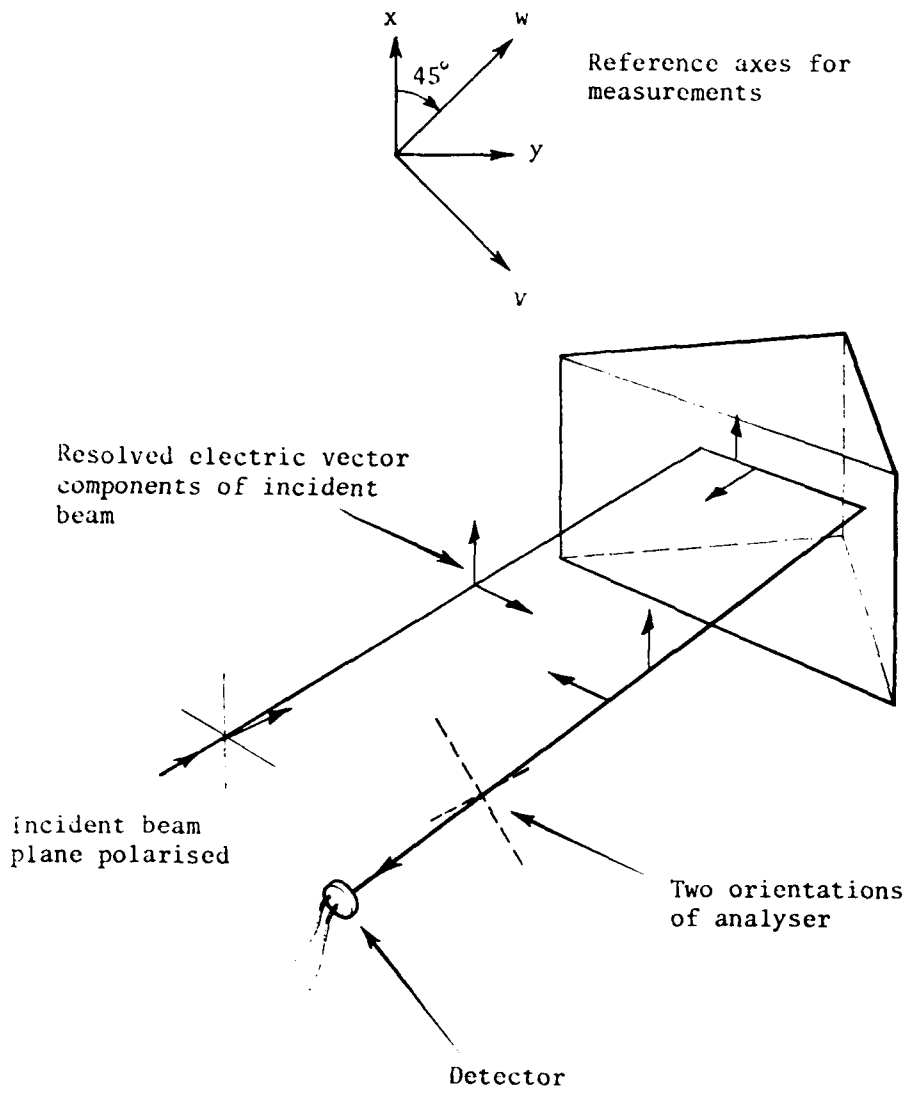


Figure 25. Layout of measurement system

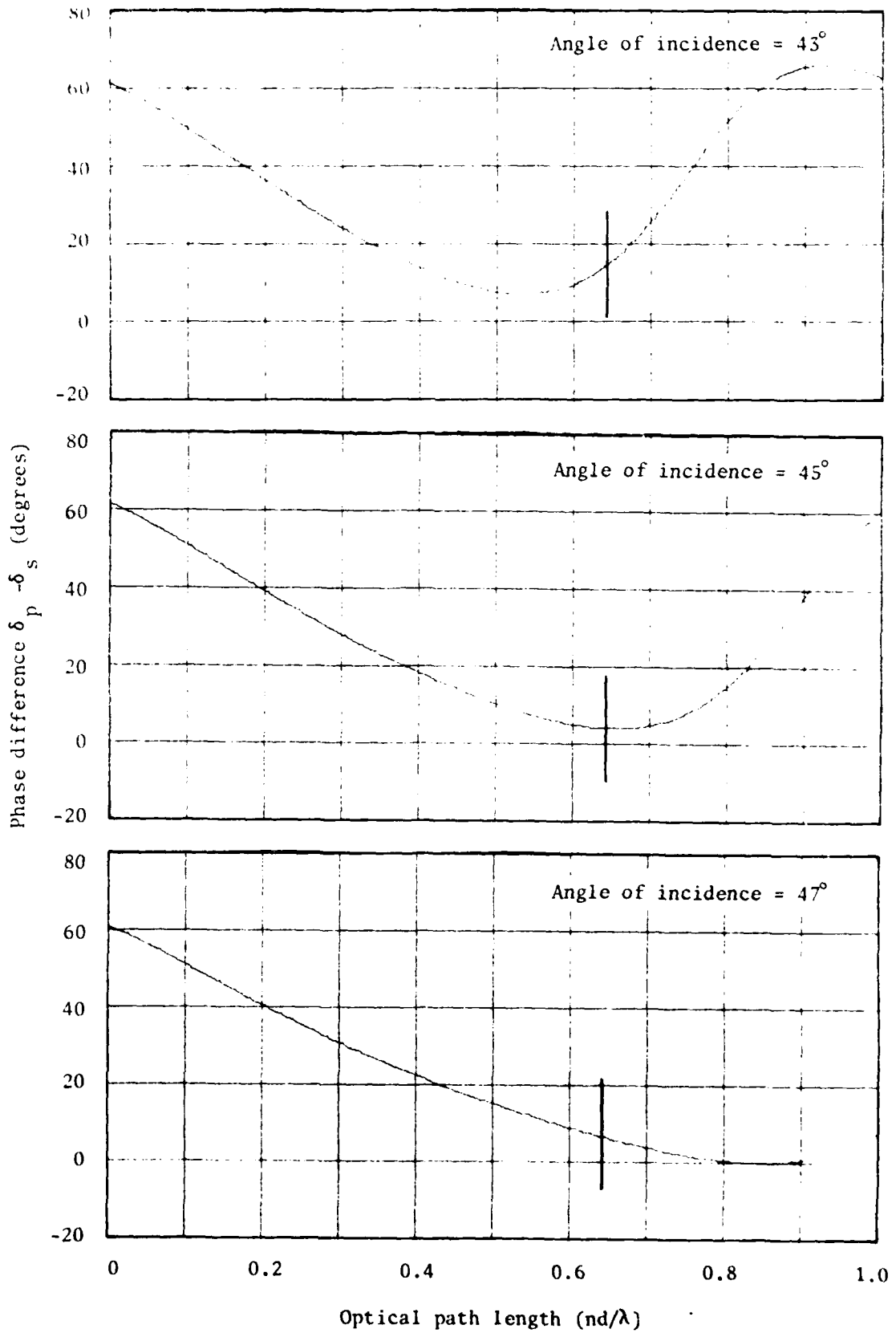


Figure 26. Variation of phase difference with variation of angle of incidence; prism index = 1.76, film index = 1.38

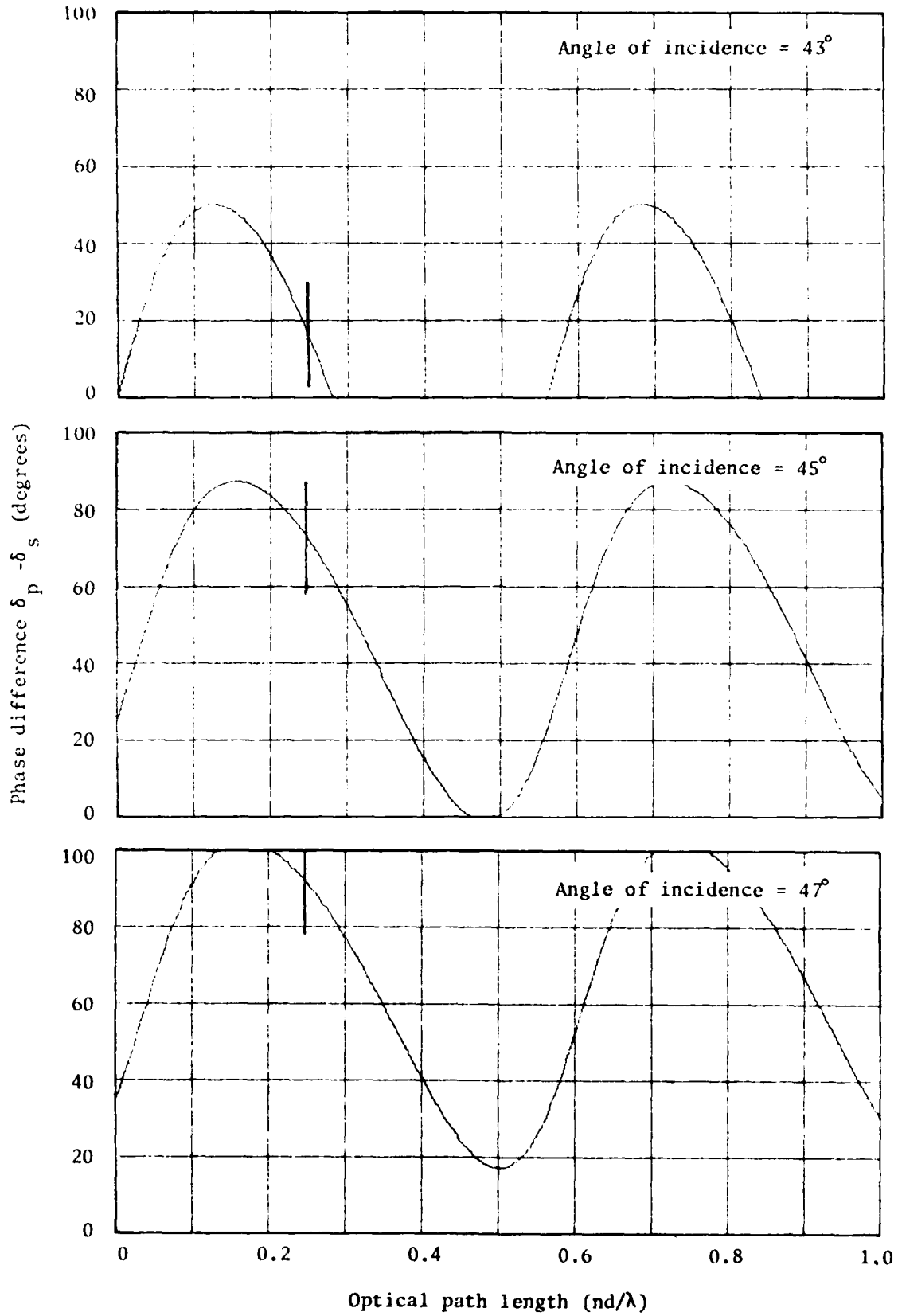


Figure 27. Variation of phase difference with variation of angle of incidence; prism index = 1.45, film index = 2.2

## DISTRIBUTION

	Copy No.
EXTERNAL	
In United Kingdom	
Defence Scientific and Technical Representative, London	No copy
British Library Lending Division, Boston Spa, Yorkshire	1
Technology Reports Centre, Orpington, Kent	2
In United States	
Counsellor, Defence Science, Washington	No copy
Engineering Societies Library, New York, NY	3
National Technical Information Services, Springfield, Va.	4
In Australia	
Chief Defence Scientist	5
Deputy Chief Defence Scientist	6
Superintendent, Science and Technology Programmes	7
Director, Joint Intelligence Organisation (DDSTI)	8
Director, Industry Development, Regional Office, Adelaide	9
First Assistant Secretary, Defence Industry and Material Policy	10
Document Exchange Centre	
Defence Information Services Branch (for microfilming)	11
Defence Information Services Branch for:	
United Kingdom, Ministry of Defence, Defence Research Information Centre (DRIC)	12
United States, Defense Technical Information Center	13 - 24
Canada, Ministry of National Defence, Defence Science Information Service	25
New Zealand, Ministry of Defence	26
Australian National Library	27
Director General, Army Development (NCO), Russell Offices, For ABCA Standardisation Officers	
UK representative, Canberra	28
US representative, Canberra	29
Canada representative, Canberra	30
New Zealand representative, Canberra	31
Mr R. Walker, Department of Physics, South Australian Institute of Technology	32
Mr W.S. Boundy, Department of Physics, South Australian Institute of Technology	33
Defence Library, Campbell Park	34
Library, Aeronautical Research Laboratories	35
Library, Materials Research Laboratories	36

Library, South Australian Institute of Technology	37
Library, University of Adelaide	38
Library, Flinders University	39

WITHIN DRCS

Chief Superintendent, Electronics Research Laboratory	40
Chief Superintendent, Advanced Engineering Laboratory	41
Superintendent, Navigation and Surveillance Division	42
Superintendent, Electronic Warfare Division	43
Superintendent, Mechanical Engineering and Workshops Division	44
Principal Officer, Optical Techniques Group	45
Principal Officer, Infrared and Optical Countermeasures Group	46
Principal Officer, Surveillance Systems Group	47
Principal Officer, Electro Optics Group	48
Principal Officer, Night Vision Group	49
Principal Officer, Electronic Workshops Group	50
Mr N.S. Bromilow, Optical Techniques Group	51
Dr D.G. Nichol, Optical Techniques Group	52
Mr M.S. Brown, Optical Techniques Group	53
Mr M.W. Rossiter, Optical Techniques Group	54
Mr D. Montgomery, Optical Techniques Group	55
Mr R.E. Galbreath, Optical Techniques Group	56
Mr W.H. Field, Optical Techniques Group	57
Mr R.J. Herbert, Optical Techniques Group	58
Dr D.M. Phillips, Surveillance Systems Group	59
Dr J. Richards, Electro Optics Group	60
Mr D. Rees, Surveillance Systems Group	61
Mr P.J. Wilsen, Surveillance Systems Group	62
Mr M.R. Meharry, Night Vision Group	63
Mr D.W. Neale, Electronic Workshops Group	64
Author	65 - 69
DRCS Library	70 - 71
Spares	72 - 81

## DOCUMENT CONTROL DATA SHEET

Security classification of this page

UNCLASSIFIED

<p>1 DOCUMENT NUMBERS</p> <p>AR Number: AR-002-593</p> <p>Series Number: ERL-0202-TR</p> <p>Other Numbers:</p>	<p>2 SECURITY CLASSIFICATION</p> <p>a. Complete Document: Unclassified</p> <p>b. Title in Isolation: Unclassified</p> <p>c. Summary in Isolation: Unclassified</p>
<p>3 TITLE</p> <p>RETROREFLECTIVE PHASE RETARDATION PRISMS</p>	
<p>4 PERSONAL AUTHOR(S):</p> <p>J.R. Venning</p>	<p>5 DOCUMENT DATE:</p> <p>June 1981</p> <p>6 6.1 TOTAL NUMBER OF PAGES 39</p> <p>6.2 NUMBER OF REFERENCES: 13</p>
<p>7 7.1 CORPORATE AUTHOR(S):</p> <p>Electronics Research Laboratory</p> <p>7.2 DOCUMENT SERIES AND NUMBER</p> <p>Electronics Research Laboratory 0202-TR</p>	<p>8 REFERENCE NUMBERS</p> <p>a. Task: DST 77/145</p> <p>b. Sponsoring Agency: OT/ERL</p> <p>9 COST CODE:</p>
<p>10 IMPRINT (Publishing organisation)</p> <p>Defence Research Centre Salisbury</p>	<p>11 COMPUTER PROGRAM(S) (Title(s) and language(s))</p>
<p>12 RELEASE LIMITATIONS (of the document):</p> <p>Approved for Public Release</p>	

Security classification of this page

UNCLASSIFIED



## 13 ANNOUNCEMENT LIMITATIONS (of the information on these pages)

No limitation

## 14 DESCRIPTORS:

a. EJC Thesaurus  
TermsPrisms  
Retroreflectors  
Optical equipment  
Electro optics  
Dielectric filmsb. Non-Thesaurus  
TermsPolarised light  
Phase retardation devices  
Waveplates  
Porro prisms

## 15 COSATI CODES:

2006

## 16 SUMMARY OR ABSTRACT:

(if this is security classified, the announcement of this report will be similarly classified)

A retro reflecting device with controlled phase retardation can be made by coating each reflecting surface of a porro prism with a single dielectric film. The amount of phase retardation is a function of the refractive index of the prism, the refractive index of the film and the film thickness. The retardation introduced can be readily controlled in the range of zero to  $\pi$  radians using readily available materials. The materials used are not birefringent. Two phase retardation prisms have been made and evaluated.

The official documents produced by the Laboratories of the Defence Research Centre Salisbury are issued in one of five categories: Reports, Technical Reports, Technical Memoranda, Manuals and Specifications. The purpose of the latter two categories is self-evident, with the other three categories being used for the following purposes:

- Reports : documents prepared for managerial purposes.
- Technical Reports : records of scientific and technical work of a permanent value intended for other scientists and technologists working in the field.
- Technical Memoranda : *intended primarily for disseminating information within the DSTO. They are usually tentative in nature and reflect the personal views of the author.*

DATE  
FILMED

4-8